Betatron Radiation Emission in plasma

EuPRAXIA School on Plasma Accelerators
24/04/2024

Alessandro Curcio (LNF INFN)

Alessandro Curcio
acurcio@lnf.infn.it

INFN
Istituto Nazionale di Fisica Nucleare

TOR VERGATA
UNIVERSITÀ DEGLI STUDI DI ROMA

Consiglio Nazionale delle Ricerche

Topics touched on

1) Laser Wakefield Acceleration (very brief introduction)

2) Electron dynamics and betatron radiation

3) Diagnostic techniques and applications of betatron radiation
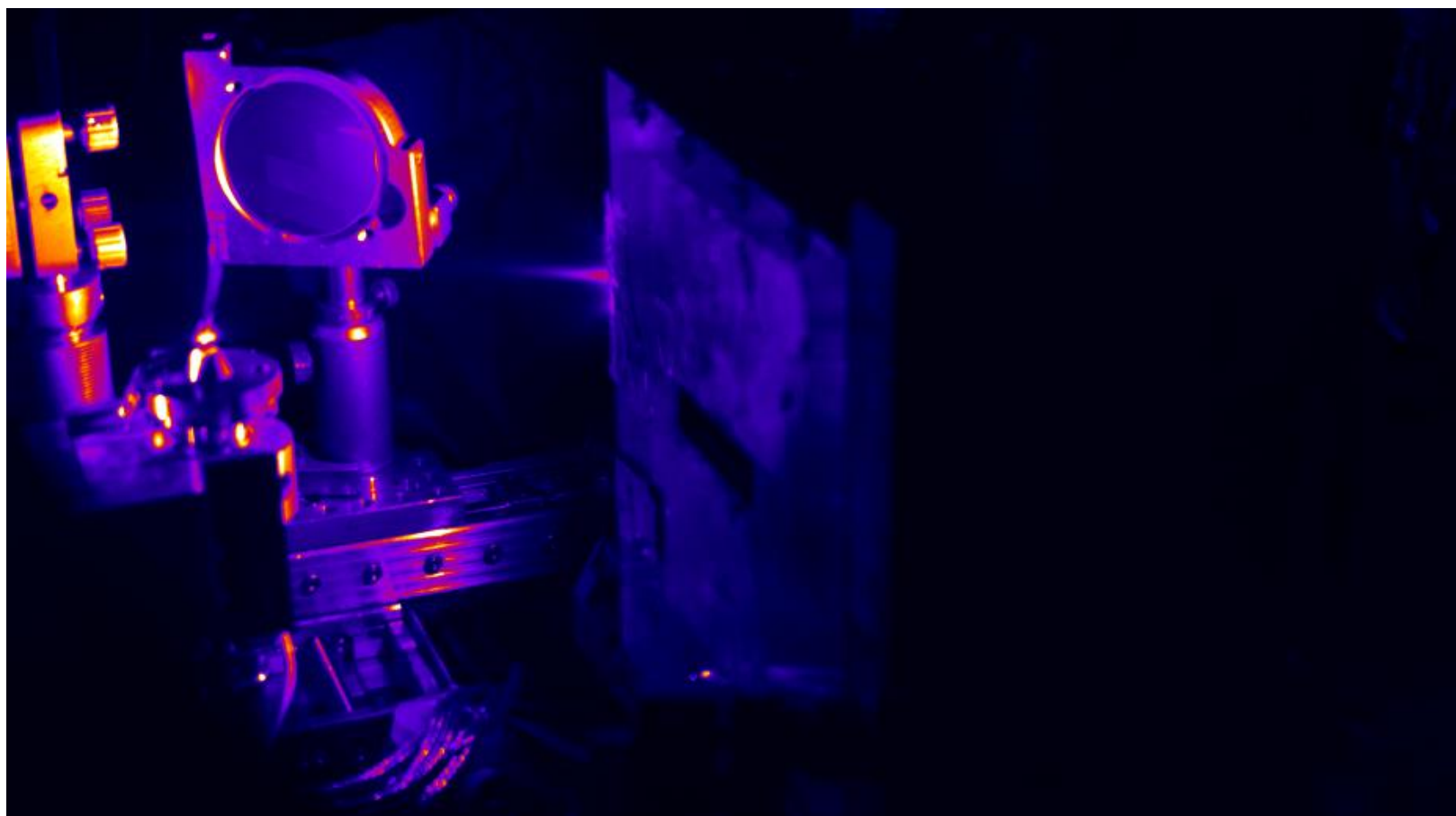
Finanziato
dall'Unione europea
NextGenerationEU

Ministero
dell'Università
e della Ricerca

Italiadomani
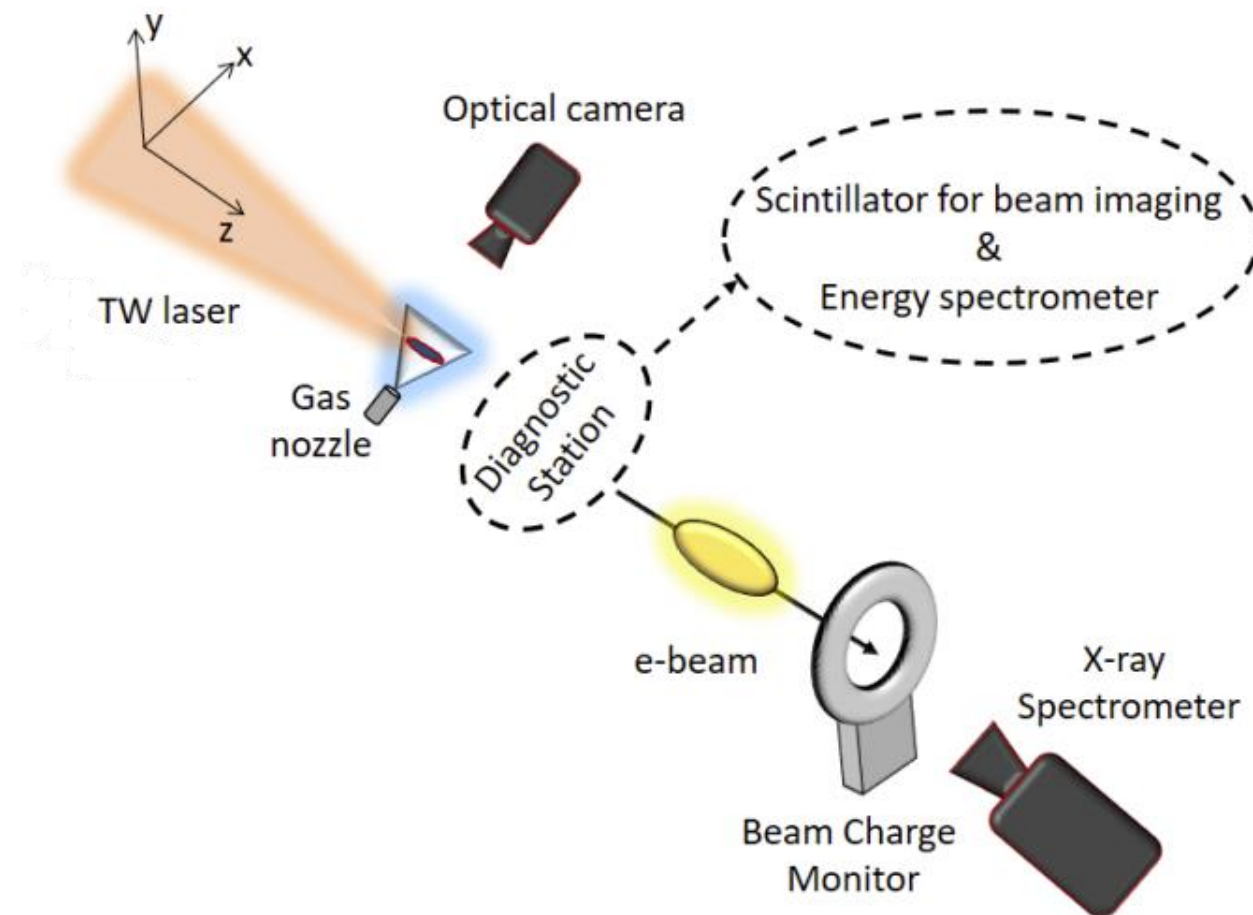PIANO NAZIONALE
DI RIPRESA E RESILIENZA

EuPRAXIA
Advanced Photon Sources

A picture of a laser-wakefield accelerator

↔ 2 mm

Typical experimental setup

A TW-class (or PW these days) laser accelerates a beam of electrons while interacting with a gas nozzle.

When the electron beam enters the energy spectrometer, consisting of a magnetic dipole (which deflects the beam out of the straight path) coupled to a scintillating screen, the X-ray detector is inserted in line with the X-ray beam, which flies on a straight line from the nozzle to the detector.

As the electron beam passes through the BCM, in a straight line, the X-ray spectrometer is moved outward.
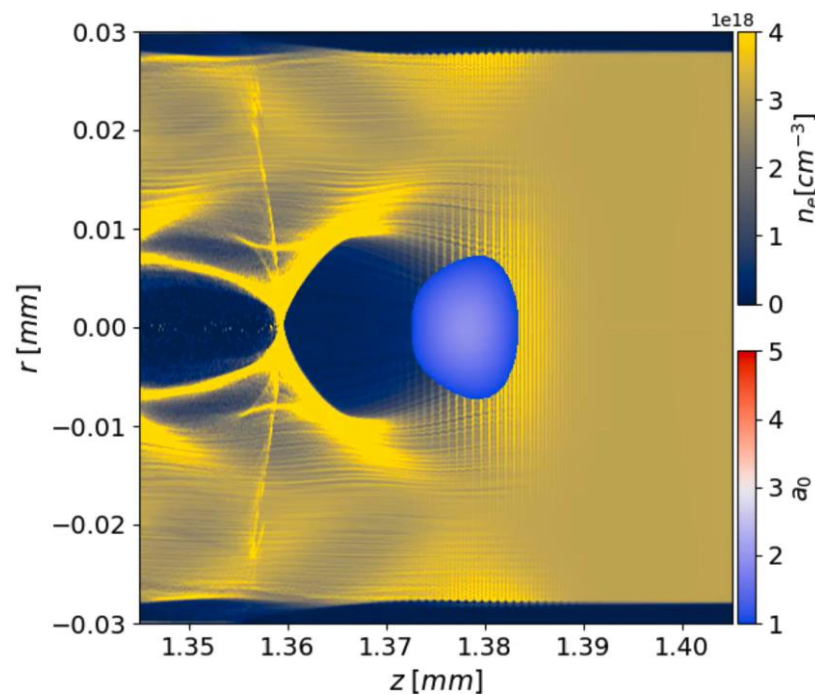
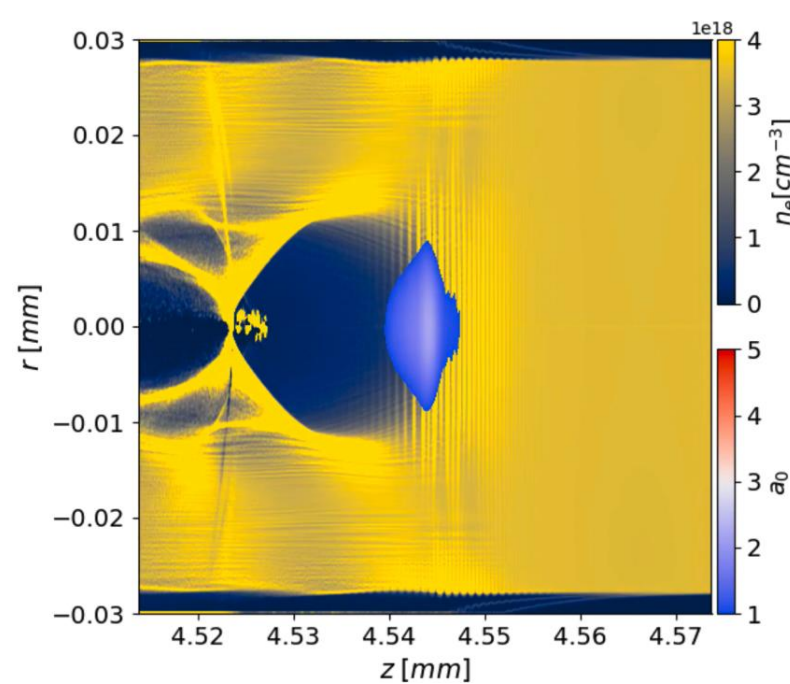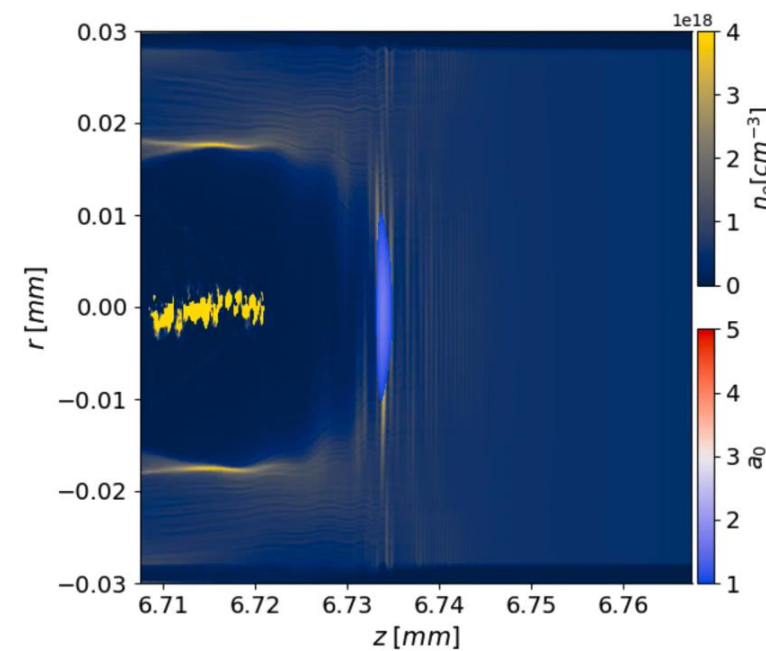# Non-linear laser-plasma wakefields: bubble regime
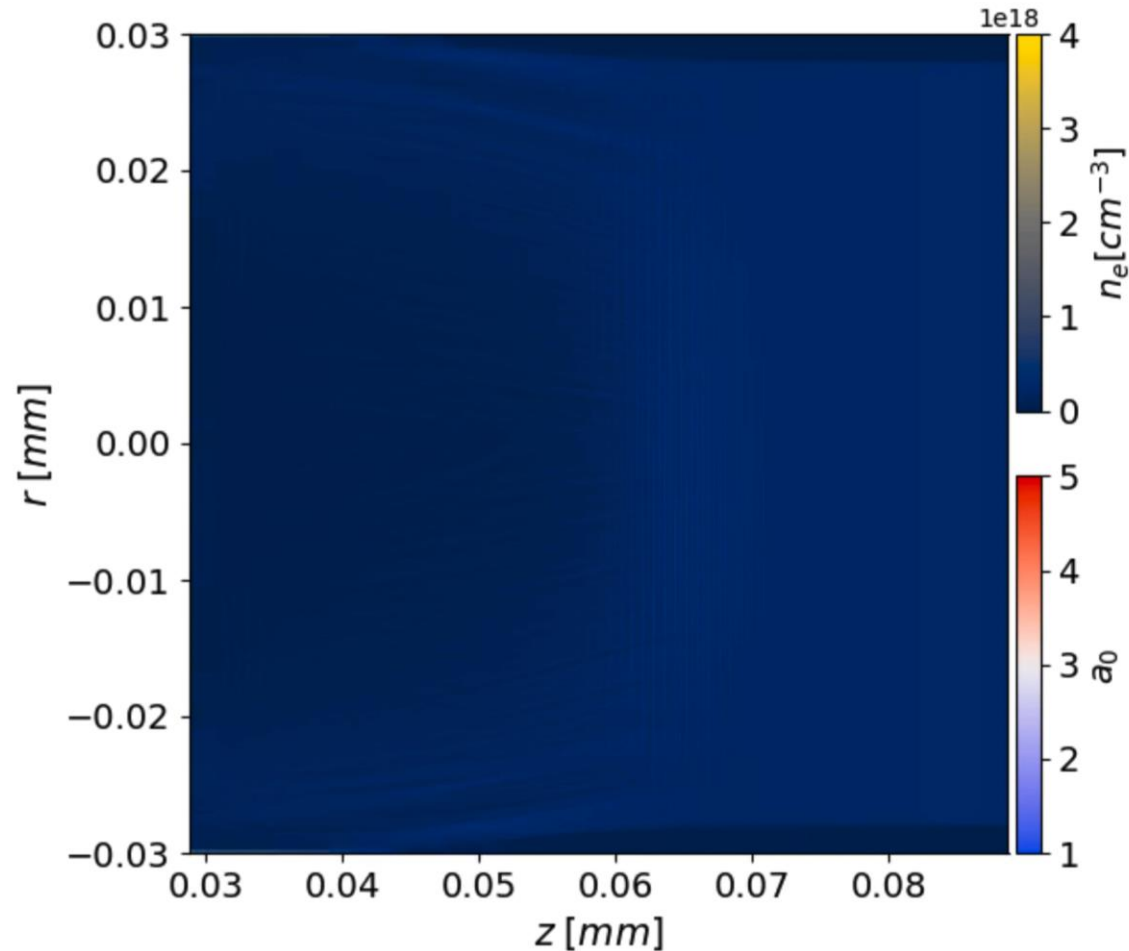
Snapshots of bubble regime

Bubble formation

Electron injection

Exit from plasma

The wakefield potential in the non-linear regime

The wakefield structure in the non-linear regime resembles to a bubble if symmetric, or even more often to an elongated ion cavity (longer than larger). A commonly used approximation is to calculate the electric potential in the ion cavity is to assume a region completely emptied of electrons (via the ponderomotive force). With the Gauss theorem we obtain:

$$\phi(\vec{r}, t) = m \frac{\omega_p^2 x^2}{4} + m \frac{\omega_p^2 y^2}{4} + m \frac{\omega_p^2 (z - ct)^2}{4}$$

The longitudinal component of the potential is expressed in z- c t, since it propagates on the wake of the laser pulse. If the laser beam undergoes to some evolution (see for example the oscillations due to self-focusing or the pump depletion, or just the wake formation) we multiply by a function of time:

$$\phi(\vec{r}, t) = \left(m \frac{\omega_p^2 x^2}{4} + m \frac{\omega_p^2 y^2}{4} + m \frac{\omega_p^2 (z - ct)^2}{4} \right) F(t)$$

The hamiltonian function for a test electron under the wakefield action is the sum of mass/kinetic energy and the potential energy:

$$H = mc^2 \sqrt{1 + \frac{p^2}{m^2 c^2}} + \phi$$

Finanziato
dall'Unione europea
NextGenerationEU

Ministero
dell'Università
e della Ricerca

Italiadomani
PIANO NAZIONALE
DI RIPRESA E RESILIENZA

EuPRAXIA
Advanced Photon Sources

A few comments on electron capture and injection

A test electron with initial energy H_0 (it can be just mass energy if it was at rest, or mass plus kinetic if the electron was in motion before the interaction with the wakefield) is injected into the wake at the time t if its final energy H(t) is negative, i.e. the electron form a kind of "bound state" with the wakefield. The condition in formulas is:

$$\int_0^t dt \frac{\partial H}{\partial t} = H(t) - H_0 < -H_0$$

If we neglect the depletion and the envelope oscillations and other evolution mechanisms, we can assume that the wake is instantaneosuly "switched on" at t=0: in this case the function F(t) is a Heaviside θ(t). We obtain for the trapping condition:

$$H(t) - H_0 = \left(m\frac{\omega_p^2 x^2}{4} + m\frac{\omega_p^2 y^2}{4} + m\frac{\omega_p^2 (z - ct)^2}{4} \right) \theta(t) + (\gamma(t) - \gamma_0) mc^2 < -\gamma_0 mc^2$$

which never gives a negative energy, i.e. never an electron injected into the wakefield!

We learn that in a self-injection of electrons into a plasma wave is related to the laser pulse dynamics, and it seems that it cannot happen just thanks to an electrostatic attraction towards the center of the ion cavity. Electrons can be injected from the cavity walls, most often this happens from the rear of the cavity, where the electron density reaches a peak, corresponding to a further potential. Moreover, another self-injection mechanism is the ionization-injection...(all this means that the above Hamiltonian misses some pieces!)
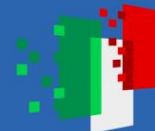
Electron dynamics and acceleration

From now on we assume that electrons are injected (there are conditions for injection), so we study their dynamics. The equations for the electron motion are in good approximation:

$$\frac{dp_x}{dt} = -\frac{m\omega_p^2 x}{2}$$

$$\frac{dp_y}{dt} = -\frac{m\omega_p^2 y}{2}$$

$$\frac{dp_z}{dt} = -\frac{m\omega_p^2 (z - ct)}{2}$$

All equations resemble the harmonic oscillator equation: the electron is attracted towards the center of the ion cavity, therefore it oscillates in x and y but also it accelerated along z, since the bubble moves at the speed of light!
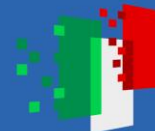
The dephasing length

An electron accelerating in the plasma wakefield is attracted to the center of the ion cavity. If the electron keeps going on its way after reaching that point, it will experience a decelerating field, in fact it will be still attracted back towards the center of the ion cavity.

The electron moves almost uniformly along z, with a trajectory z = v t, while the laser moves approximately at speed of light, at its group velocity v_g.

When the path difference between the electron and the laser is equal to R (bubble radius), i.e. when the electron is at the center of the ion cavity, we say that the electron enters the dephasing region. In formulas:
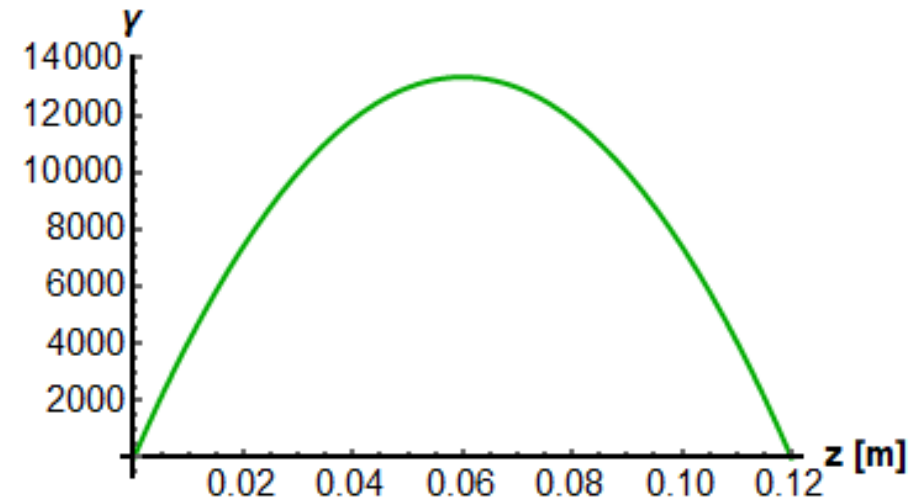
$$\beta_e \simeq 1 \qquad L_{deph} = \frac{cR}{(c - v_g)} \sim \frac{4}{3} \frac{\omega_0^2}{\omega_{p0}^2} \frac{\sqrt{a_0}}{k_{p0}} \qquad \beta_g = \frac{d\omega}{dk} = \frac{c\,d\omega}{d(n\omega)} = \frac{c}{n + \omega \frac{dn}{d\omega}}$$

Being the radius R comparable to the laser beam radius (of the order of several microns or few tens of microns), and being ω_0 hundreds times ω_p for typical experimental conditions, we get that the dephasing length is of the order of several mm.

Finanziato
dall'Unione europea
NextGenerationEU

Ministero
dell'Università
e della Ricerca

Italiadomani
PIANO NAZIONALE
DI RIPRESA E RESILIENZA

EuPRAXIA
Advanced Photon Sources

The energy gain

$$\gamma \simeq \gamma_{max} \left[1 - \left(1 - \frac{\gamma_0}{\gamma_{max}} \right) \left(\frac{t}{t_d} - 1 \right)^2 \right]$$
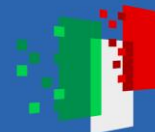

For what we said about the dephasing, we can model the Lorentz factor in a parabolic way.
This allows solving the electron motion analytically, even if it's not the rigorous way.
In the above example, for rather extreme parameters, an electron is accelerated up to 7 GeV over 6 cm.
The maximal Lorentz factor parameter can be found as the product of the average accelerating field from the rear of the ion cavity to the dephasing point times the dephasing length:

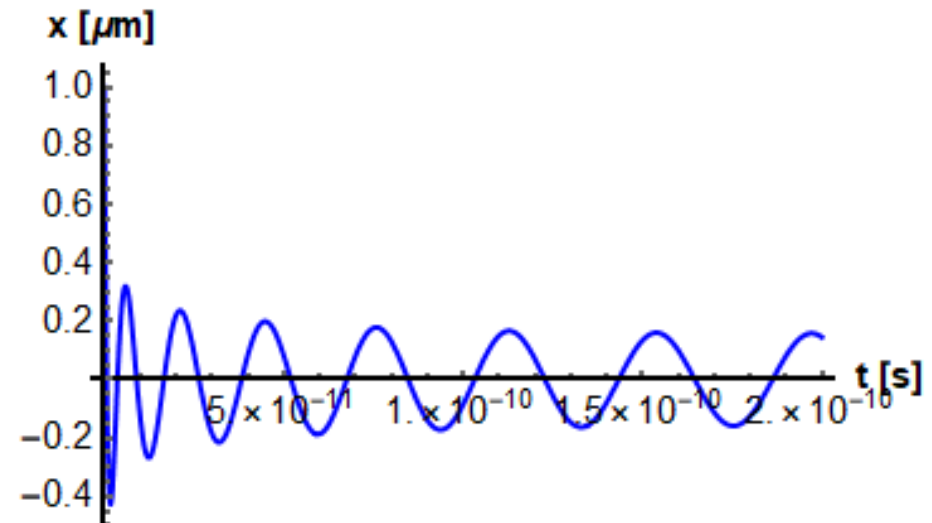$$\gamma_{max} = \frac{2}{3} a_0 \frac{\omega_0^2}{\omega_{p0}^2}$$

Betatron dynamics

$$\frac{dp_x}{dt} = -\frac{m\omega_p^2 x}{2}$$

$$\frac{dp_y}{dt} = -\frac{m\omega_p^2 y}{2}$$

$$\frac{dp_z}{dt} = -\frac{m\omega_p^2(z - ct)}{2}$$

$$\gamma \simeq \gamma_{max}\left[1 - \left(1 - \frac{\gamma_0}{\gamma_{max}}\right)\left(\frac{t}{t_d} - 1\right)^2\right]$$
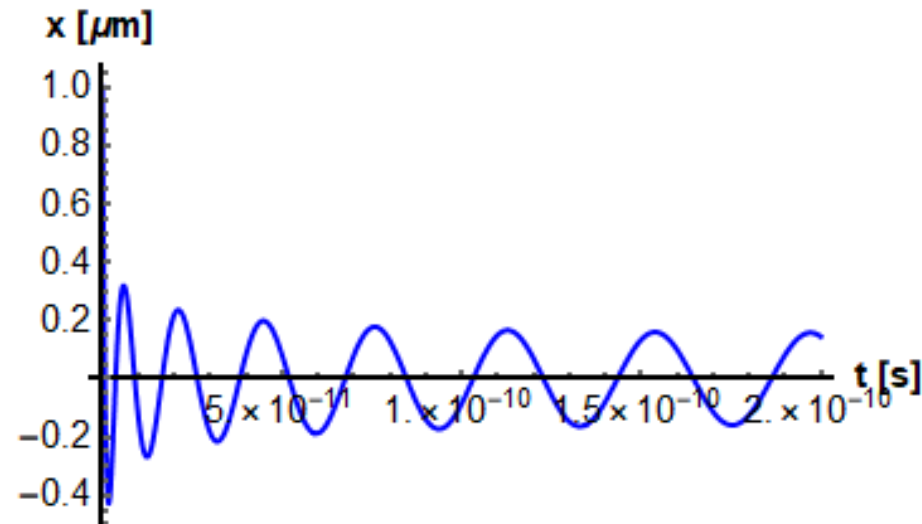
With the previous definition of parabolic Lorentz factor (as function of the time), the solution for the x and y motion is oscillatory. Being the electrons known as beta particles, such oscillations are also known as betatron oscillations (from betatron, an old type of electron accelerator). We have seen these oscillations in the PIC image.

Here above we also see that the amplitude of these oscillations is damped from few microns to a fraction of microns in normal conditions of operation.
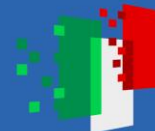
Finanziato
dall'Unione europea
NextGenerationEU

Ministero
dell'Università
e della Ricerca

Italiadomani
PIANO NAZIONALE
DI RIPRESA E RESILIENZA

EuPRAXIA
Advanced Photon Sources

Betatron oscillations

The analytic expression of the above oscillations with the parabolic Lorentz factor is in terms of Legendre polynomials. We see that after a transient time, the period and the amplitude of betatron oscillations stabilize. This happens when the electrons become approach the dephasing point, which also coincides with the maximum energy gain.
Therefore, in good approximation, close to the point of maximum energy gain, we get:

$$x(t) \simeq x_0 \cos\left(\omega_\beta t + \phi_x\right)$$

$$\omega_\beta \simeq \frac{\omega_p}{\sqrt{2\gamma_{max}}}$$

Betatron Oscillations: a picture from PIC simulations
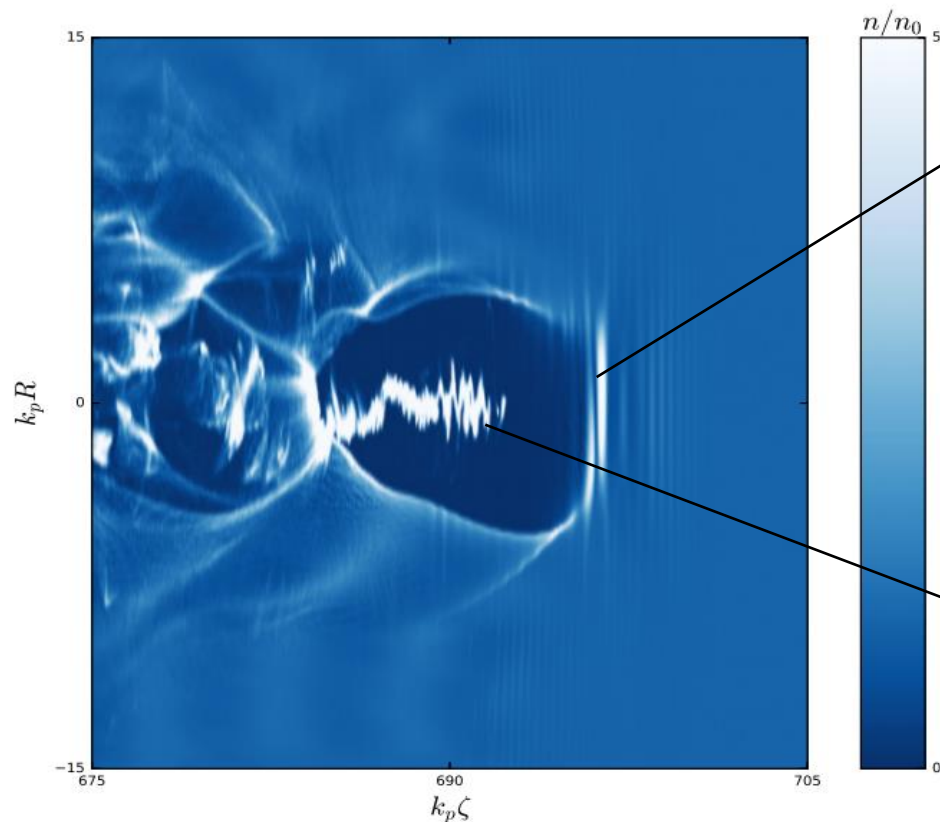
Laser propagating in the underdense plasma: a cavitation region free of electrons is created on its wake. The latter is called plasma ion cavity, responsable for electron acceleration and focusing

Electrons injected into the plasma bubble wiggling while accelerating: this is at the base of the emission of Betatron Radiation

Electron dynamics: a bit more in detail

$$x = x_\beta(t) \sin \left(\int \omega_\beta(t)dt + \psi_x + \varphi_0 \right)$$

$$y = y_\beta(t) \sin \left(\int \omega_\beta(t)dt + \psi_y + \varphi_0 \right)$$

Legendre polynomials can be approximated as here on the left. The electron trajectories resemble those in a magnetic wiggler. Differently from a wiggler the oscillation amplitude and frequency depend upon time. Furthermore, each electron corresponds to a different initial amplitude (position of injection) : this will bring to a inhomogeneous broadening of the radiation spectrum.

$$z = \int_0^t v_z dt$$

$$\omega_\beta(t) = \frac{\omega_p}{\sqrt{2\gamma(t)}}$$

$$v_z \simeq c \left(1 - \frac{1}{2\gamma^2(t)} - \frac{\omega_\beta^2(t)}{2c^2} \left[x_\beta^2(t) \cos^2 \left(\int \omega_\beta(t)dt + \psi_x + \varphi_0 \right) + y_\beta^2(t) \cos^2 \left(\int \omega_\beta(t)dt + \psi_y + \varphi_0 \right) \right] \right)$$

Similarly as in undulators, wigglers and FELs, longitudinal dynamics is retarded due to the coupling with transverse oscillations. This also defines the so-called undulator parameter, which red-shifts the resonant frequency of radiation.
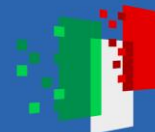
Radiation from bent particles
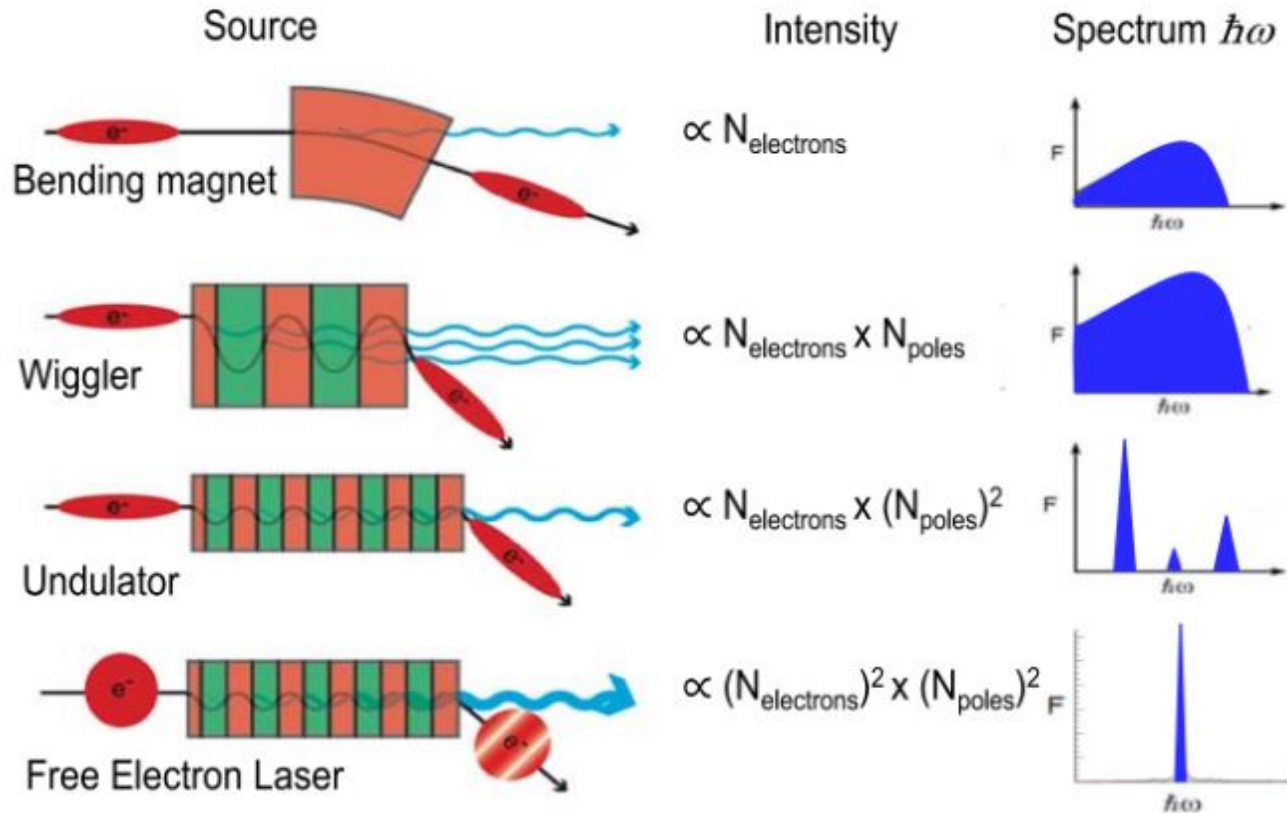
It is often said that betatron radiation resembles to the case of the wiggler:

Forward radiation is mostly emitted at the curvature points of the electron oscillating trajectories, where each turning point acts (in terms of radiation) as a bending magnet (corresponding to synchrotron radiation)

How true is this?

The final answer will be that betatron radiation is a mix of undulator and wiggler radiation
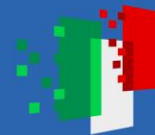
The undulator strength parameter(s)

$$K_x(t) = \frac{\gamma(t)\omega_\beta(t)x_\beta(t)}{c}$$

$$K_y(t) = \frac{\gamma(t)\omega_\beta(t)y_\beta(t)}{c}$$

As customary, we distinguish different radiation regimes according to the strength of the undulator parameter.

For K<<1 or K~1 the undulator regime is realized.

For K>>1 the wiggler regime is realized.

How similar is betatron radiation to synchrotron radiation? Inhomogeneous broadening is the key to answer.

Many electrons realize the wiggler conditions, due to betatron oscillations with relatively large amplitude.

However, many other electrons (often the majority), propagate on-axis (especially for on-axis injection case), i.e. correspond to small betatron oscillation amplitudes and thus to small strength parameters (undulator regime).

Despite being the majority, on-axis electrons emit less efficiently (we'll show this): the final photon number can be determined both by off and on-axis electrons, i.e. as wiggler and undulator radiation (broadened).

Ref.
Esarey, E., et al. "Synchrotron radiation from electron beams in plasma-focusing channels." *Physical Review E* 65.5 (2002).

Different regimes of radiation: undulator-like

$$\omega_n(t,\theta) = \frac{2\gamma^2 n \omega_\beta(t)}{2\gamma^2(t)\left\langle\frac{1+\gamma^2\theta^2}{2\gamma^2}\right\rangle_t + \frac{K_\beta^2(t)}{2}}$$

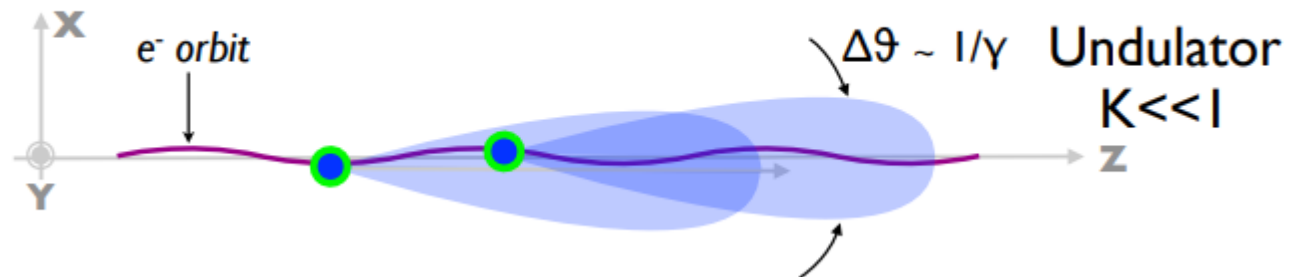$$K_\beta^2(t) = K_x^2(t) + K_y^2(t)$$

From the on-axis electrons undulator radiation is expected, but with different efficiency, since more violent is the oscillation, more photons are emitted.

At relatively large K (still <1) inhomogeneous red-shift is realized.

Indeed, the number of emitted photons can be estimated via the Larmor law, being for the undulator case:

$$N_\gamma(t) \propto K_\beta^2(t)$$

Refs.
Corde, Sébastien, et al. "Femtosecond x rays from laser-plasma accelerators." *Reviews of Modern Physics* 85.1 (2013): 1.

Different regimes of radiation: wiggler-like

$$\omega_x(t) = \frac{3\gamma^2 K_\beta^4 \omega_\beta}{2K_x^3}\left(1+\frac{K_y^2}{2K_x^2}\right)^{-3/2} \propto \gamma^{7/4}(t)$$

$$\omega_y(t) = \frac{3\gamma^2 K_\beta^4 \omega_\beta}{2K_y^3}\left(1+\frac{K_x^2}{2K_y^2}\right)^{-3/2} \propto \gamma^{7/4}(t)$$
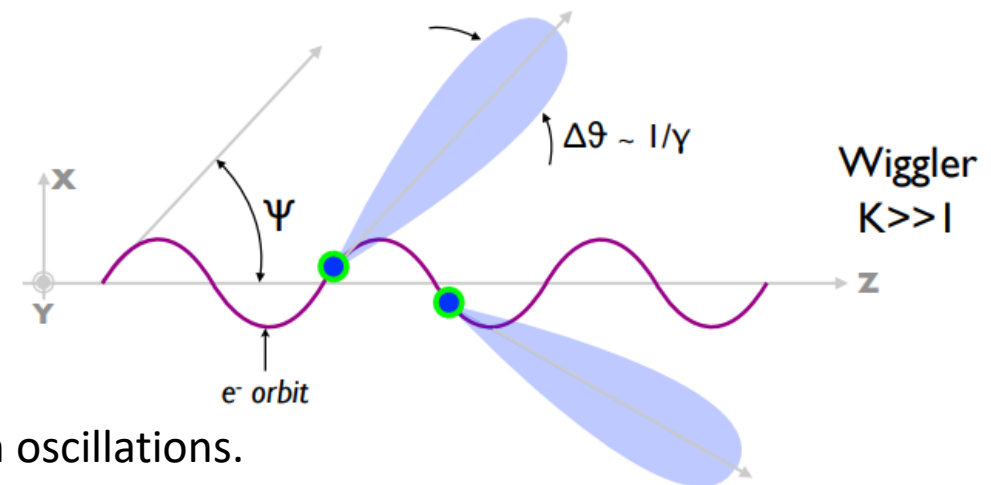
Two different critical frequencies are defined for the two planes of betatron oscillations.

The wiggler spectrum resembles a synchrotron spectrum.

Synchrotron-like betatron radiation is associated only with electrons of the bunch such to have large K (>>1) parameters.

$$N_\gamma(t) \propto K_\beta(t)$$

Betatron radiation divergence

$$\theta_x(t) = \frac{1}{\gamma(t)}$$

$$\theta_y(t) = \frac{1}{\gamma(t)}$$

Betatron radiation divergence in the undulator regime, i.e. divergence of the radiation emitted by on-axis electrons of the bunch. The symbol of equality is an approximation.
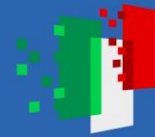
$$\theta_x(t) = \frac{K_x(t)}{\gamma(t)}$$

$$\theta_y(t) = \frac{K_y(t)}{\gamma(t)}$$

Betatron radiation divergence in the undulator regime, i.e. divergence of the radiation emitted by off-axis electrons of the bunch. The symbol of equality is an approximation.

Ref.
Rousse, Antoine, et al. "Production of a keV X-ray beam from synchrotron radiation in relativistic laser-plasma interaction." *Physical review letters* 93.13 (2004): 135005.

Inhomogeneous broadening

- Plasma bubbles act accelerating but also focusing.

- Focusing fields are quasi-electrostatic.

- In a magnetic undulator the strength parameter is approximately the same for all electrons and depends only on physical constants and the magnetic field.

- The strength parameter in a plasma focusing cannel is different for each electron and depends on the oscillation amplitude, leading to inhomogeneous broadening of the radiation spectrum and to a suppression of strong spectral-angular correlations (due to disorder).

- Another cause for inhomogeneous broadening is surely the energy spread but this is common to both a magnetic undulator and a plasma focusing cannel.

Spectral-angular correlations

$$\omega_n(t,\theta) = \frac{2\gamma^2 n \omega_\beta(t)}{2\gamma^2(t)\left\langle \frac{1+\gamma^2\theta^2}{2\gamma^2} \right\rangle_t + \frac{K_\beta^2(t)}{2}}$$

Undulator regime:
Radiation emission from on-axis electrons is suppressed. Electrons with relatively large K (still <1) can emit different frequencies at same angle due to inhomogeneous broadening (also related to energy spread).

$$\omega_x(t) \simeq \frac{3\gamma^2 K_x \omega_\beta}{2}\left(1 - \frac{3K_y^2}{4}\right) \propto \gamma^{7/4}(t)$$

$$\omega_y(t) \simeq \frac{3\gamma^2 K_y \omega_\beta}{2}\left(1 - \frac{3K_x^2}{4}\right) \propto \gamma^{7/4}(t)$$

Wiggler regime:
Radiation is surely more relevant for off-axis electrons; spectral-angular correlation is anyway spoiled by inhomogeneous broadening, since at the same observation angle electrons with different strength parameter (and kinetic energy) contribute to the radiation spectrum and yield.
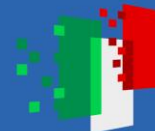
Theoretical model of betatron radiation

Betatron Trajectories

$$x(t) = x_\beta(t) \cos\left(\int_0^t \omega_\beta(t')dt' + \psi_x\right)$$

$$y(t) = y_\beta(t) \cos\left(\int_0^t \omega_\beta(t')dt' + \psi_y\right)$$

$$z(t) \simeq \int_0^t \left[1 - \frac{1}{2\gamma^2(t')} - \frac{1}{2c^2}\left(\frac{dx}{dt'}\right)^2 - \frac{1}{2c^2}\left(\frac{dy}{dt'}\right)^2\right]dt'$$

Magnetic Field component of the Radiation Field

$$\vec{H}(\theta, \phi, \omega) = \frac{i\omega}{4\pi c}\frac{e^{i\frac{\omega R}{c}}}{R^2}\vec{R} \times \widetilde{\vec{j}}(\vec{k}, \omega)$$

Spectral-Angular distribution of Radiated Energy

$$\frac{d^2E}{d\omega d\Omega} = \frac{\omega^2}{16\pi^3\varepsilon_0 c^3}\left[\widetilde{j}_x^2 + \widetilde{j}_y^2 + \widetilde{j}_z^2\theta^2 - 2\widetilde{j}_z(\widetilde{j}_x\cos\phi + \widetilde{j}_y\sin\phi)\theta\right]$$

Resonance function

$$R_n(t) = \frac{i - ie^{i\left[\left(\left\langle\frac{1+\gamma^2\theta^2}{2\gamma^2}\right\rangle_t + \frac{K_\beta^2(t)}{4\gamma^2(t)}\right)\omega - n\langle\omega_\beta\rangle_t\right]t}}{\left(\left\langle\frac{1+\gamma^2\theta^2}{2\gamma^2}\right\rangle_t + \frac{K_\beta^2(t)}{4\gamma^2(t)}\right)\omega - n\langle\omega_\beta\rangle_t}$$

Radiation Currents

$$\widetilde{j}_x = \frac{q}{2}\sum_{\alpha,n,\mu,\nu}\int_0^t x_\beta\,\omega_\beta\left(J_{\alpha+2\mu}\left(\rho_x^{(1)}\right)\left[J_{n-\alpha+2\nu+1}\left(\rho_y^{(1)}\right) + J_{n-\alpha+2\nu-1}\left(\rho_y^{(1)}\right)\right]J_\mu\left(\rho_x^{(2)}\right)J_\nu\left(\rho_y^{(2)}\right)R_n'e^{-i\alpha\psi_x - i(n-\alpha)\psi_y}\right)dt'$$

$$\widetilde{j}_y = \frac{q}{2}\sum_{\alpha,n,\mu,\nu}\int_0^t y_\beta\,\omega_\beta\left(J_{\alpha+2\mu}\left(\rho_x^{(1)}\right)\left[J_{n-\alpha+2\nu+1}\left(\rho_y^{(1)}\right) + J_{n-\alpha+2\nu-1}\left(\rho_y^{(1)}\right)\right]J_\mu\left(\rho_x^{(2)}\right)J_\nu\left(\rho_y^{(2)}\right)R_n'e^{-i\alpha\psi_x - i(n-\alpha)\psi_y}\right)dt'$$

$$\widetilde{j}_z = qc\sum_{\alpha,n,\mu,\nu}\int_0^t J_{\alpha+2\mu}\left(\rho_x^{(1)}\right)J_{n-\alpha+2\nu}\left(\rho_y^{(1)}\right)J_\mu\left(\rho_x^{(2)}\right)J_\nu\left(\rho_y^{(2)}\right)R_n'e^{-i\alpha\psi_x - i(n-\alpha)\psi_y}dt'$$

Finanziato
dall'Unione europea
NextGenerationEU

Ministero
dell'Università
e della Ricerca

Italiadomani
PIANO NAZIONALE
DI RIPRESA E RESILIENZA

EuPRAXIA
Advanced Photon Sources

Betatron radiation: asymptotic currents and critical frequency, planar trajectory and fixed observation angle

$$\tilde{j}_x \simeq \left\langle 4iex_\beta \sqrt{N_\beta} \frac{(1+\gamma^2\theta^2)}{\sqrt{3}K_\beta} K_{2/3}\left(\frac{\omega}{2\omega_c}\right) \right\rangle_t$$

$$\tilde{j}_z \simeq \left\langle -4ec\frac{\sqrt{N_\beta}}{\omega_\beta} \frac{\sqrt{1+\gamma^2\theta^2}}{\sqrt{3}K_\beta} K_{1/3}\left(\frac{\omega}{2\omega_c}\right) \right\rangle_t$$

$$\omega_c(t) \simeq \frac{3\gamma^3(t)\omega_\beta^2(t)x_\beta(t)}{2c\left(1+\gamma^2(t)\theta^2\right)^{3/2}}$$

Asymptotic expressions of the Bessel functions for $K_\beta \gg 1$

Case of only horizontal current (planar trajectory)

Observation angle: vertical

Other cases are difficult to treat analytically

Critical frequency appearing as in synchrotron radiation!
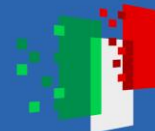
Betatron radiation: Synchrotron-like spectrum

$$\frac{d^2E}{d\omega d\Omega}(t) \simeq \frac{4\hbar\alpha\omega^2}{3\pi^2}\left(\left\langle \frac{(1+\gamma^2\theta^2)\sqrt{N_\beta}}{\gamma\omega_\beta K_\beta}K_{2/3}\left(\frac{\omega}{2\omega_c}\right)\right\rangle_t^2 + \left\langle \frac{\sqrt{1+\gamma^2\theta^2}\sqrt{N_\beta}}{\omega_\beta K_\beta}\theta K_{1/3}\left(\frac{\omega}{2\omega_c}\right)\right\rangle_t^2\right)$$

The time average is related to acceleration

Currents/fields are averaged, not intensity!

Comparison with synchrotron radiation formula:

$$\frac{d^2E}{d\omega d\Omega} = \frac{\hbar\alpha\omega^2\rho^2}{3\pi^2 c^2}\left(\frac{1+\gamma^2\theta^2}{\gamma^2}\right)^2\left(K_{2/3}^2(\xi) + \frac{\gamma^2\theta^2}{1+\gamma^2\theta^2}K_{1/3}^2(\xi)\right) \qquad \xi = \left(\frac{\omega\rho}{3\gamma^3 c}\right)(1+\gamma^2\theta^2)^{3/2}$$

Apparently very similar, but no dependence on time, which red-shifts significantly the spectrum, and remember that the Betatron radiation formula above is specialized for planar horizontal trajectory and vertical observation angle, otherwise…

Direct energy-scaling and spectral density comparison

Betatron Radiation

Synchrotron Radiation

$$\omega_x(t) \simeq \frac{3\gamma^2 K_x \omega_\beta}{2}\left(1 - \frac{3K_y^2}{4}\right) \propto \gamma^{7/4}(t)$$

Critical frequency
On-axis

$$\omega_c \propto \gamma^3$$

$$\omega_y(t) \simeq \frac{3\gamma^2 K_y \omega_\beta}{2}\left(1 - \frac{3K_x^2}{4}\right) \propto \gamma^{7/4}(t)$$

$$P(t) \propto \gamma^{3/2}(t)$$ Peak

Power

$$P \propto \gamma^4$$ Mean

Cumbersome expression, where Bessel K functions are integrated upon time.
No appearance of Bessel K 5/3.
This brings to an enhancement of low-frequency photons compared to Synchrotron Radiation spectrum (effect of the acceleration).

Spectral Density

$$S = \frac{9\sqrt{3}\omega}{8\pi\omega_c}\int_{\omega/\omega_c}^{\infty} K_{5/3}(x)\,dx$$
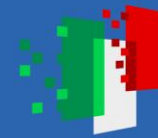
Temporal incoherence of betatron radiation
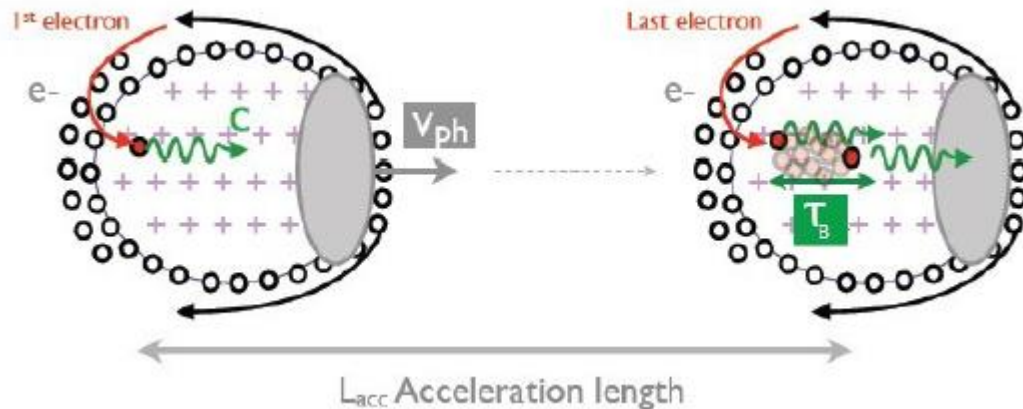
$$\tau_B = L_{deph} \frac{c - v_\phi}{c^2}$$

Assuming continuous injection until the dephasing point, we obtain an electron bunch length which is comparable to the radius of the plasma bubble.

At first approximation the betatron radiation pulse length is equal to the electron bunch length.

For typical plasma densities used in self-injection experiments, bubble radii are of the order of few microns to tens of microns.

Electron bunches are too long to emit coherently in the X-rays.

Ref.
Ta Phuoc, K., Fitour, R., Tafzi, A., Garl, T., Artemiev, N., Shah, R., ... & Kostyukov, I. (2007). Demonstration of the ultrafast nature of laser produced betatron radiation. *Physics of Plasmas*, *14*(8), 080701.

Temporal properties of betatron radiation
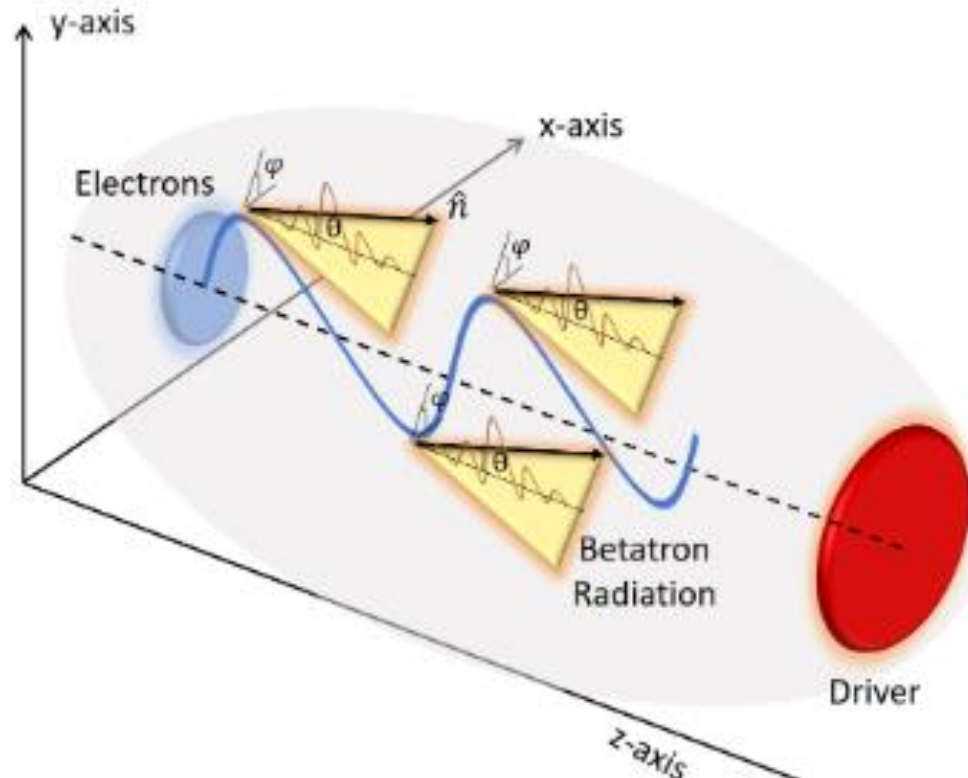
$$\tau_{rms}^2 = \int d\omega \left(\frac{d|S(\omega)|}{d\omega} \right)^2 + \int d\omega |S(\omega)|^2 \left(\frac{d\phi}{d\omega} \right)^2$$

Same duration of the electron bunch?
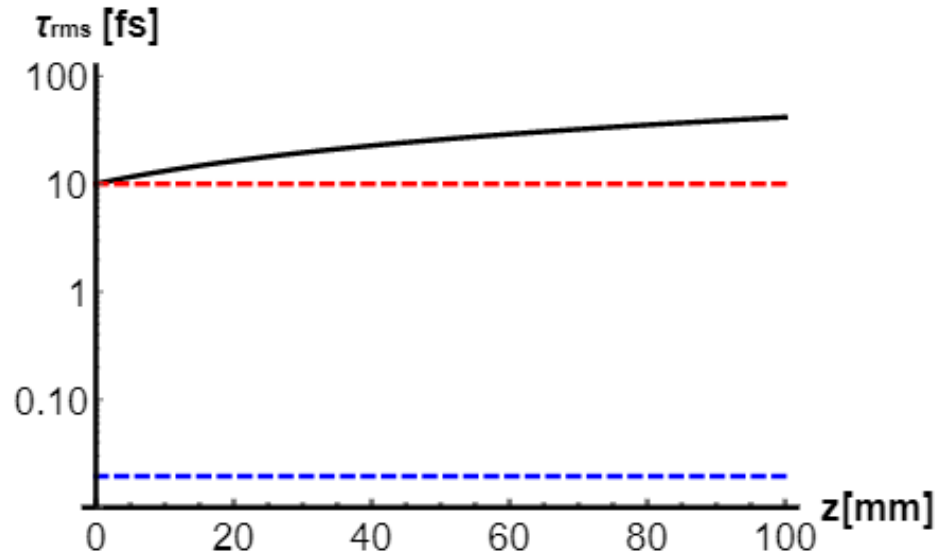
$$\tau_{rms}(z) = \tau_e + \frac{\epsilon}{c} + \frac{\hat{\theta}_\beta^2 z}{2c}$$

Comparison between the betatron pulse (black line) stretching during propagation in a vacuum, and the contribution from the bunch length (dashed red) and from the beam emittance (dashed blue) at the source level.
Used parameters: emittance = 3.9 nm, bunch length = 10 fs, electron plasma density ne = 10x19 cm−3, finally γ = 300, i.e. beam divergence equal to 10 mrad.

Ref. Curcio, A., and G. Gatti. "Time-domain study of the synchrotron radiation emitted from electron beams in plasma focusing channels." *Physical Review E* 105.2 (2022): 025201.

Betatron X-ray chirp
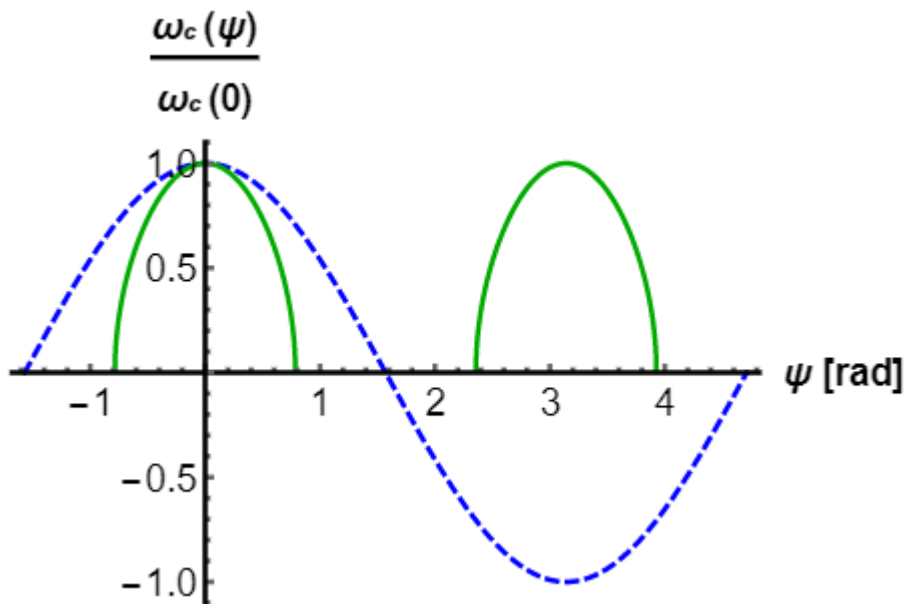
$$\omega_c(\psi) = \frac{3}{2}\gamma^3\omega_\beta\theta_\beta f(\psi)$$

$$f^2(\psi) = \cos(2\psi)$$
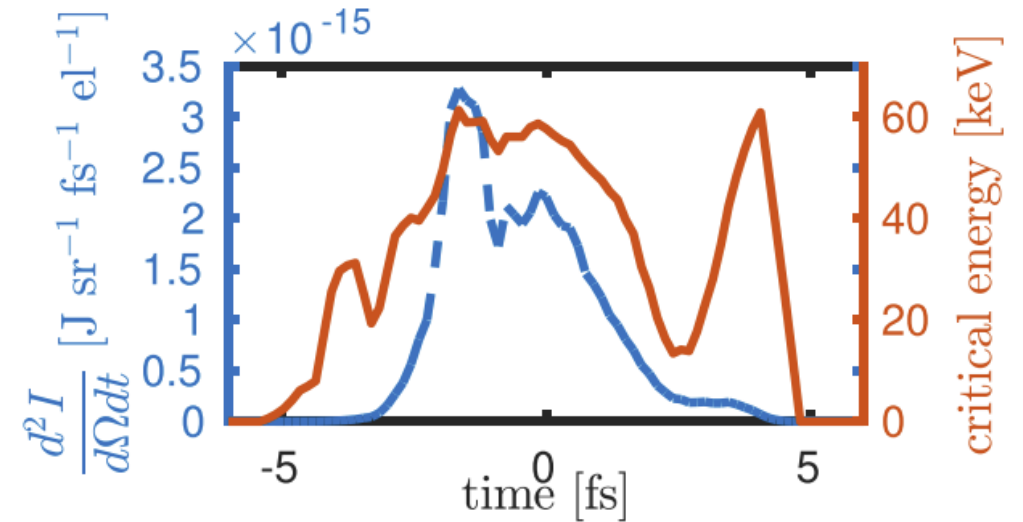
Betatron X-rays are chirped, the amount of chirp being related to the bunch length and to the symmetry of the plasma wave/electron pulse.

Ref. Horný, Vojtěch, et al. "Temporal profile of betatron radiation from laser-driven electron accelerators." *Physics of Plasmas* 24.6 (2017).
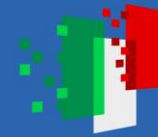
EuPRAXIA Advanced Photon Sources Proposal

EuAPS Scientific Coordinator:
M. Ferrario (INFN-LNF)
EuPRAXIA/EuAPS Integration:
R. Assmann (DESY & INFN)

Milano
Milano
Pisa
Frascati/Roma
Potenza
Catania

WP1
MANAGEMENT & DISSEMINATION
A. Falone (LNF)

WP3
HIGH POWER LASER BEAM LINE
P. Cirrone (LNS)

WP2
BETATRON RADIATION SOURCE
A. Cianchi (Uni-ToV)

WP4
HIGH REPETITION RATE LASER BEAM LINE
L. Labate (CNR)
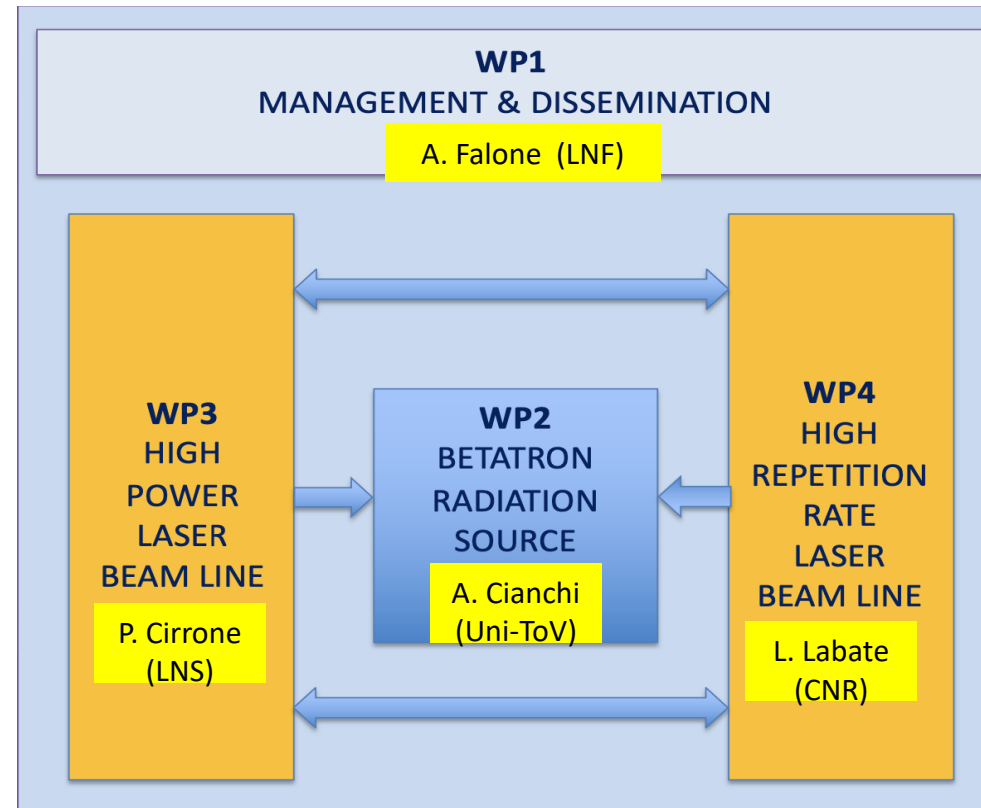
EuAPS got the highest score among IR

I 3.1, Fund for the creation of an integrated system of research and innovation infrastructures
Action 3.1.1 " Creation of new IR or strengthening of existing IR involved in the Horizon Europe Scientific Excellence objectives and the establishment of networks "

Graduatoria definitiva ESFRI area: PSE - Physical Sciences and Engineering

Position	Proposal code	Applicant	Eligible costs	Total Score	Reduction %
1	EuAPS	INFN	22.350.588,00 €	191	-17.6
2	I-PHOQS		50.000.000,00 €	188	-16.7
3	LNGS	INFN	20.058.826,53 €	185	-19.0
4	K3NET	INFN	67.186.973,06 €	183	-13.0
5	IR0000027		75.165.077,53 €	182	-21.1
6	IR0000037	ISPRA	16.671.850,52 €	181	-12.5
7	IR0000012	INAF	71.477.540,83 €	181	-19.9
8	IRIS	INFN	59.996.968,15 €	180	-20.0

EuPRAXIA Timeline
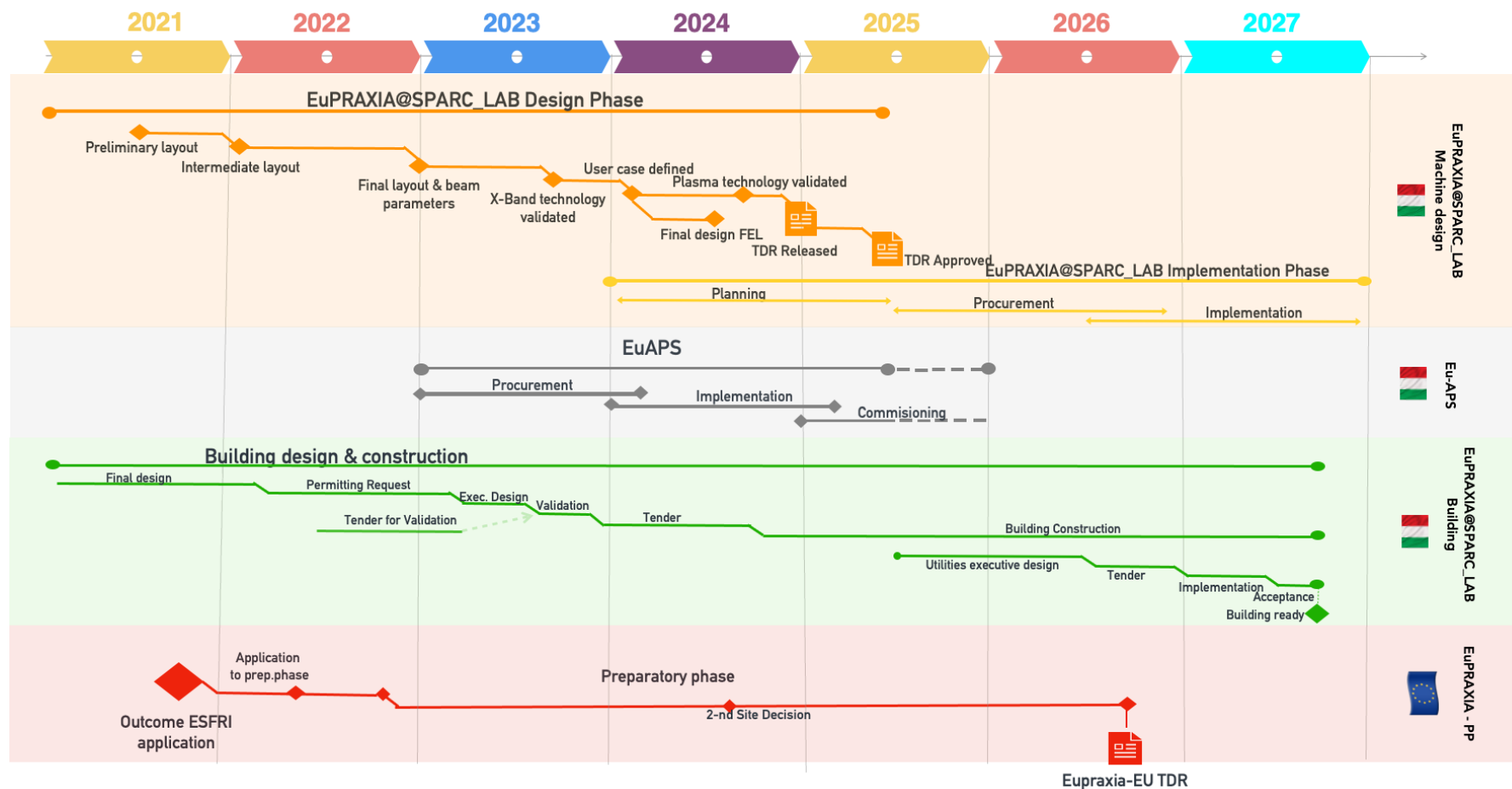
WP4 - J-class, 100Hz laser infrastructure @CNR-INO Pisa

Underground bunker

100 Hz

Intense Laser Irradiation Laboratory
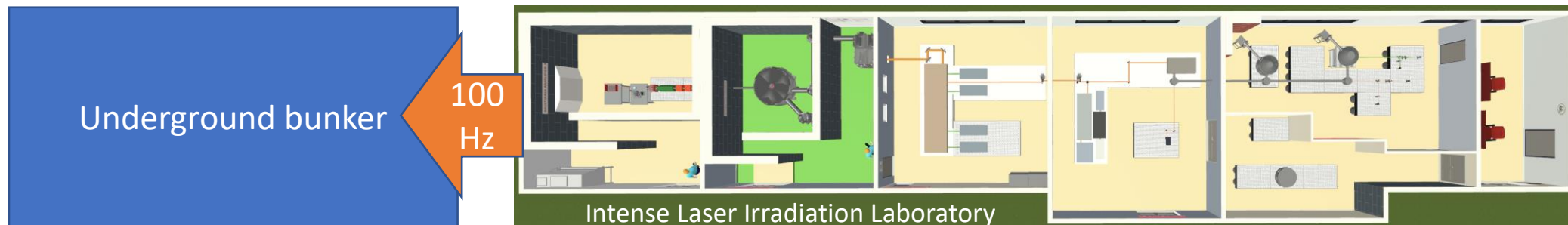
New bunker
Designed for high
dose irradiation
(100 Hz)
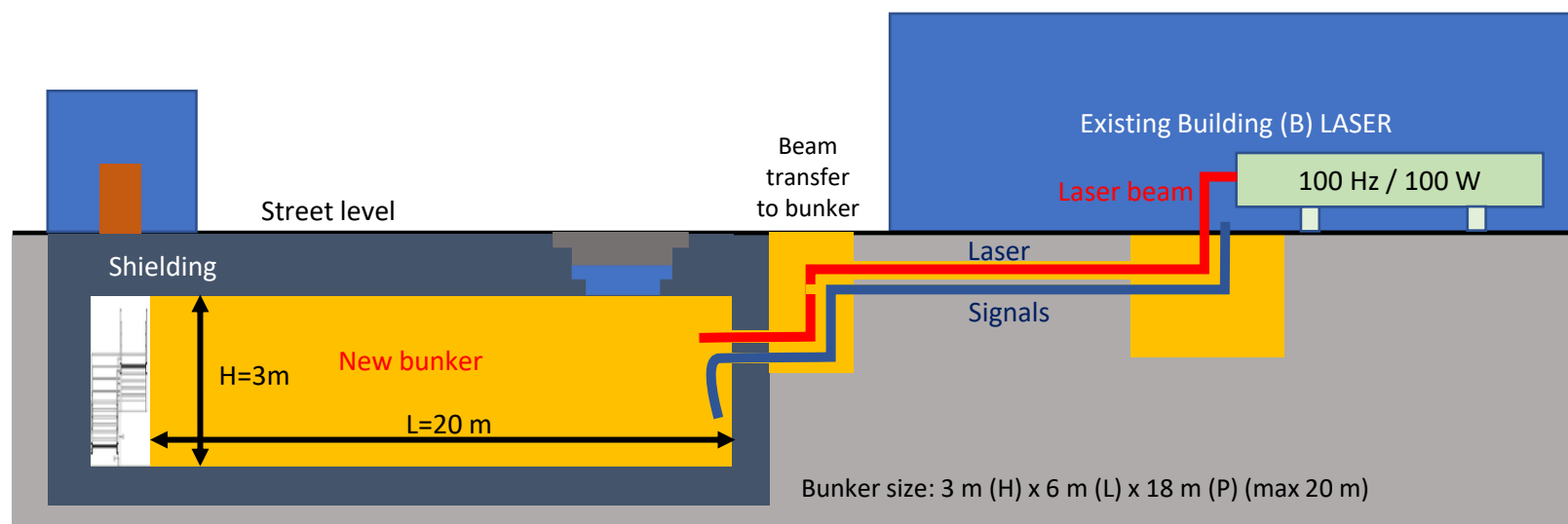
Existing Building (B) LASER

Beam
transfer
to bunker

Laser beam

100 Hz / 100 W

Street level

Laser

Signals

Shielding

New bunker

H=3m

L=20 m

Bunker size: 3 m (H) x 6 m (L) x 18 m (P) (max 20 m)

CNR-INO
ISTITUTO NAZIONALE DI OTTICA
CONSIGLIO NAZIONALE DELLE RICERCHE

Part of the IPHOQS (ELI/LENS/CUSBO Photonics Infrastructure), and Tuscan Health Ecosystem 4.5 M€ dedicated funding @ CNR-Pisa)

WP3 - I-LUCE (INFN-Laser indUced radiation acceleration)

Laser system

Utility room

Optical compressor

Interaction chamber II:
Warm Dense Matter, nuclear physics, conventional beam-plasma interaction, etc.

Interaction chamber I:
protons, ions, electrons, neutrons production

Laser path

Conventional ions:
from TANDEM and Cyclotron

In-air irradiation station

LNS

The FLAME laser at INFN-LNF
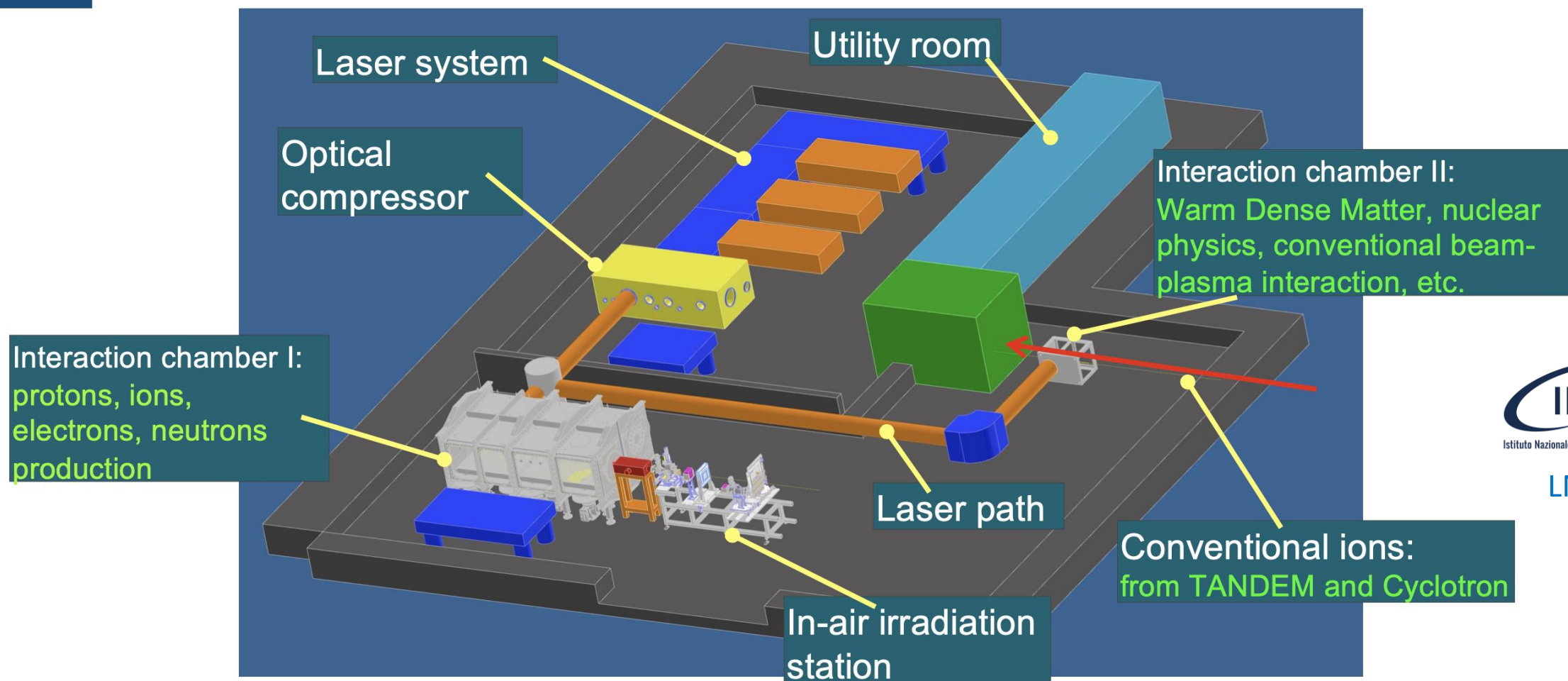
Betatron Radiation for Imaging

B. Guo et al. Sci. Rep. 2019
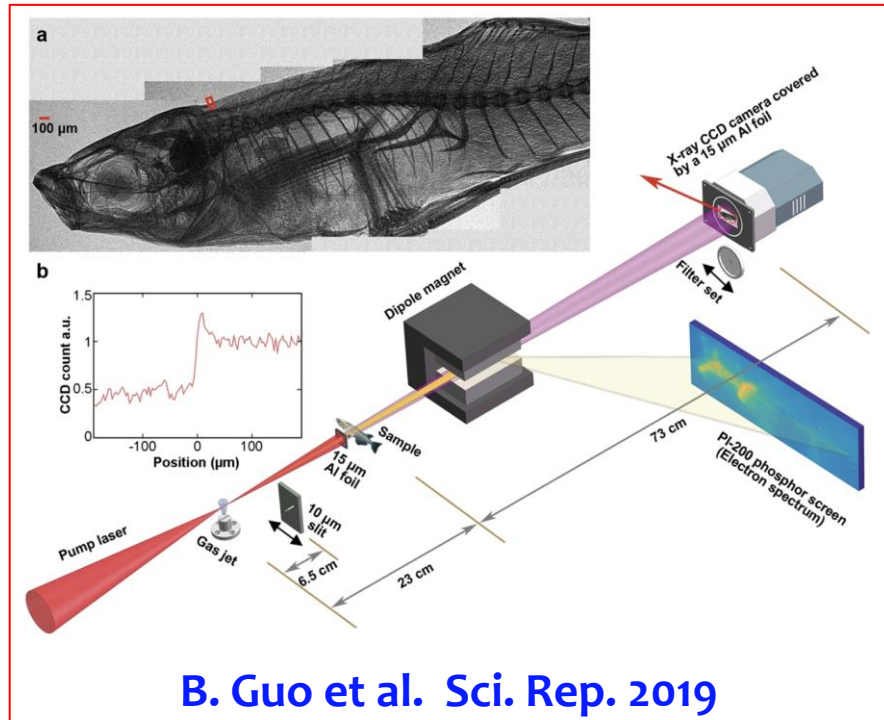
High-resolution phase-contrast imaging-XPCI of biological specimens using a stable betatron X-ray source.

Imaging at EuAPS
1) static
2) time resolved
3) related to laser induced dynamics.
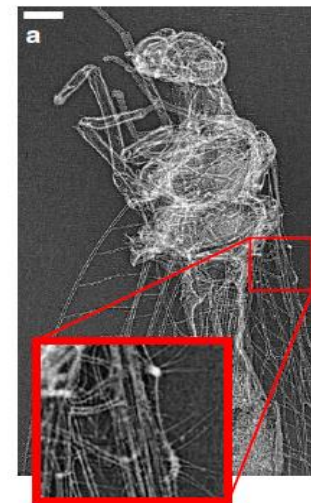
J. Wenz *et al.* Nature Comm. 2015

Micro-tomography - Bet. Rad.
J. M. Cole *et al.* PNAS 2018

Betatron Radiation for Spectroscopy
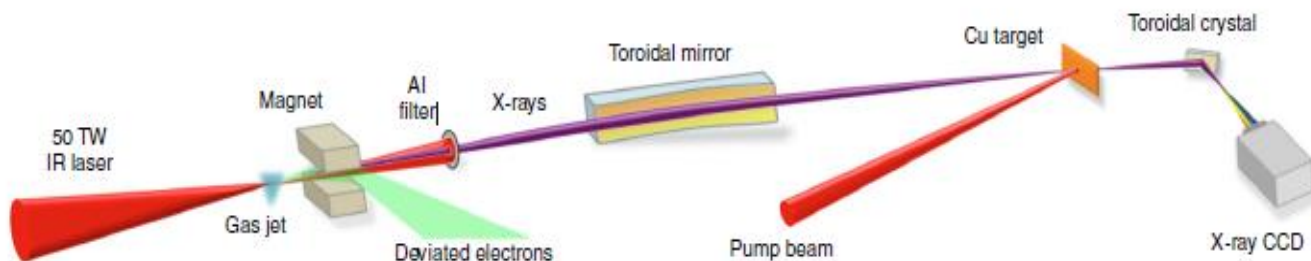
Laser-excited dynamics in metals
B. Mahieu *et al.* Nature Comm. 2018

Static or time-resolved or pump-probe material science studies at atomic scale

Cu L edges
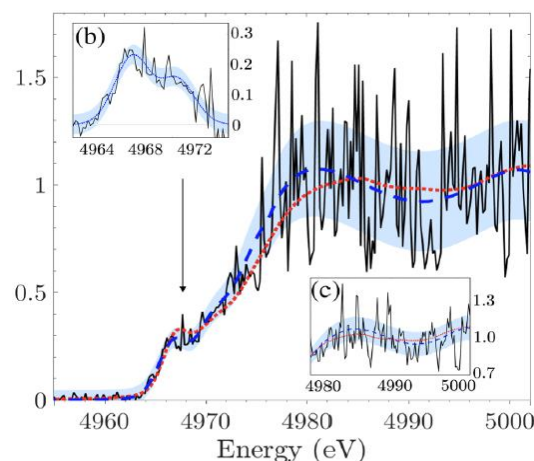
Single-shot absorption measurements on Titanium
B. Kettle *et al. Phys Rev Lett* 2019

XES XRF K$_\beta$ lines
M. Holden Rev. Sci. Instrum. 2017

Material Science Applications: Warm Dense Matter (WDM)
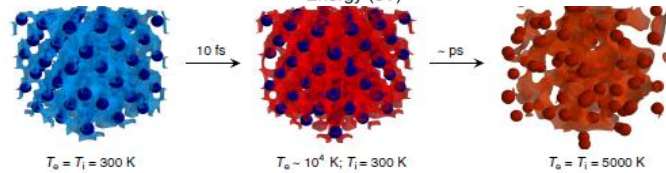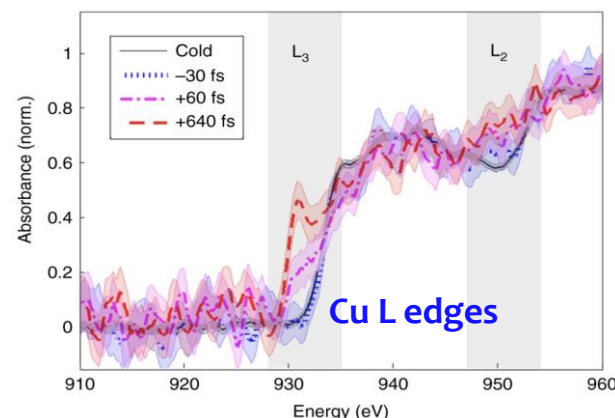
Mahieu, B., et al. "Probing warm dense matter using femtosecond X-ray absorption spectroscopy with a laser-produced betatron source." *Nature Communications* 9.1 (2018): 3276.
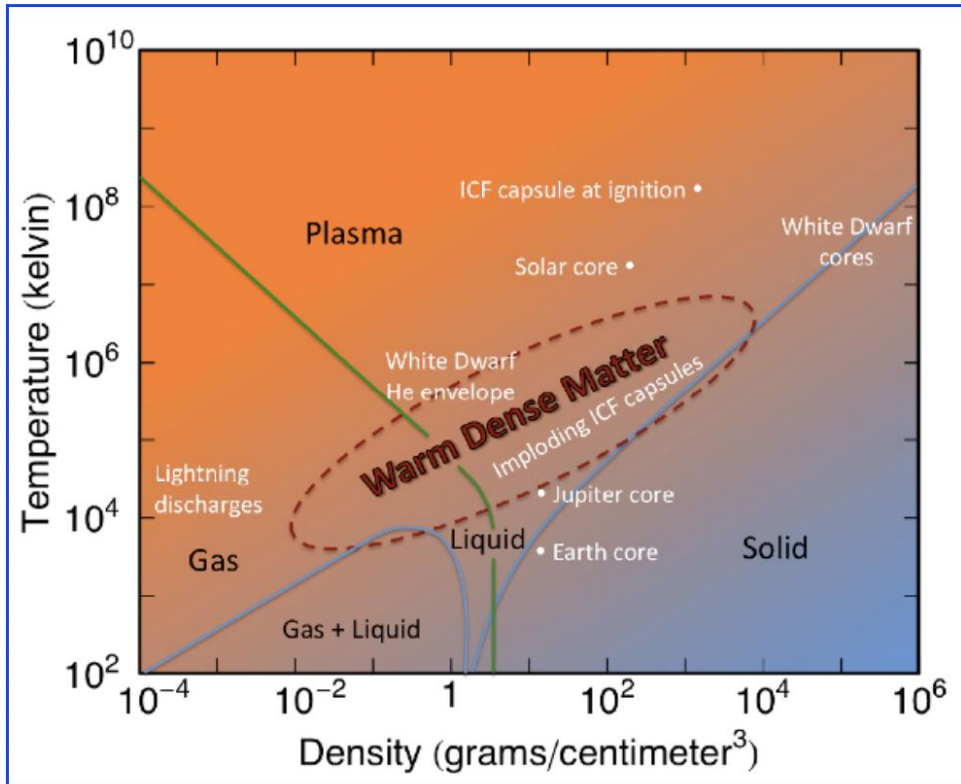
WDM occurs in:
- **Cores of large planets;**
- **Systems that start solid and end as a plasma;**
- **X-ray driven inertial fusion implosion (aspects of indirect-drive inertial fusion).**

The **investigation of such warm dense matter (WDM) is one of the great challenges of contemporary physics**.

Femtosecond lasers can rapidly heat matter, leading to ultrafast solid-liquid-WDM transitions, followed by a more complex **multiphase expansion at a picosecond time scale**. Highly nonequilibrium states of matter are expected, due to the finite rate of energy transfer from the excited electrons to the lattice.

As the atomic structure modification is supposed to be driven by the photoexcited electrons, it is of primary importance to determine the respective time scales of the evolution of both electron and atomic structures.

Electron beam divergence measurements @FLAME
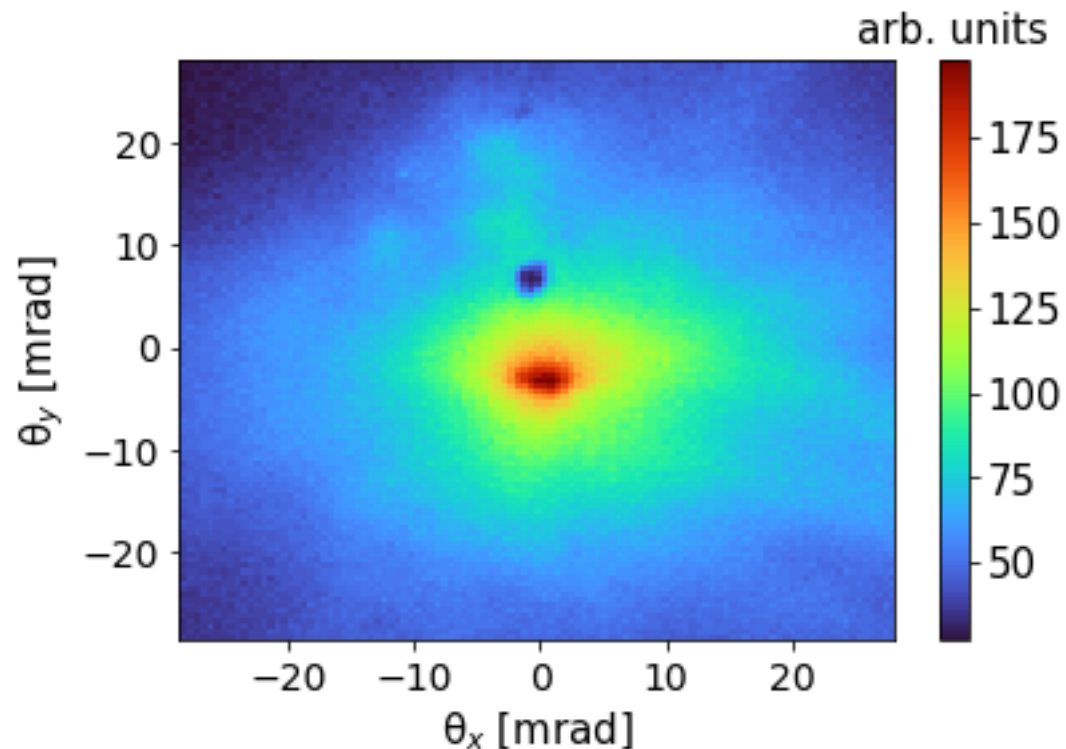
When the electron beam is not sent to the dipole and dispersed, it is detected on a scintillator screen (Lanex) where the divergence is characterized out of the source.

The best divergence we have got has been 30 mrad FWHM

Measured electron parameters @FLAME

- Electron maximum energy 300 MeV

- Bunch charge 200 pC

- Beam divergence 30-60 mrad

Average Electron Spectrum

$Q = (218 \pm 54)$ pC
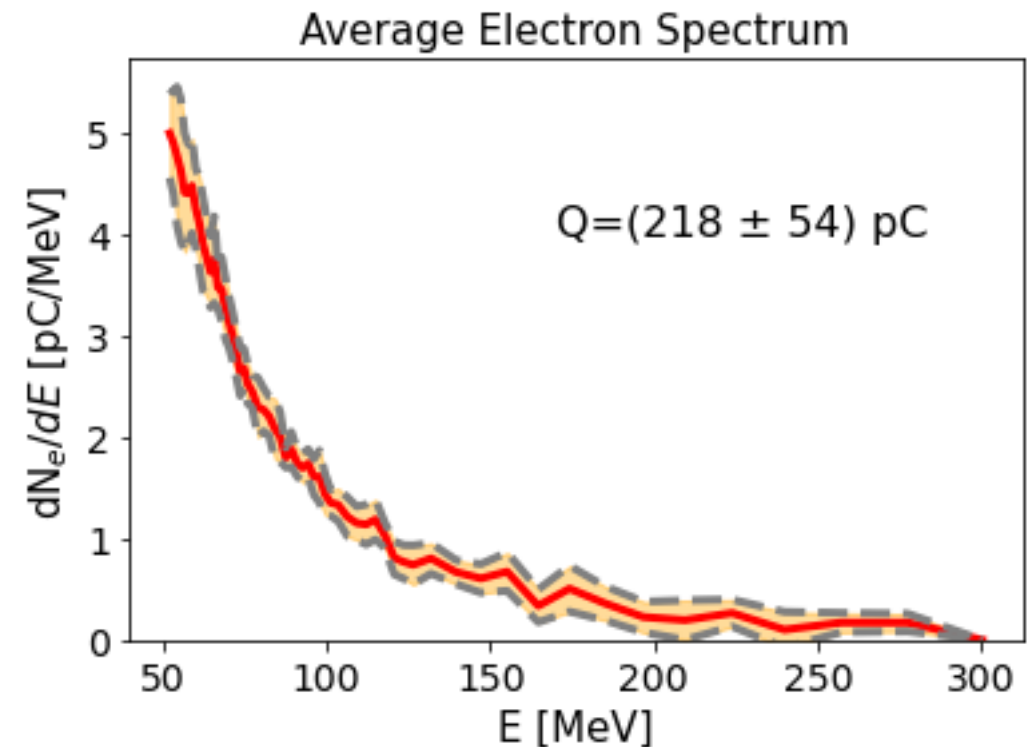
Electron-plasma density measurements @FLAME
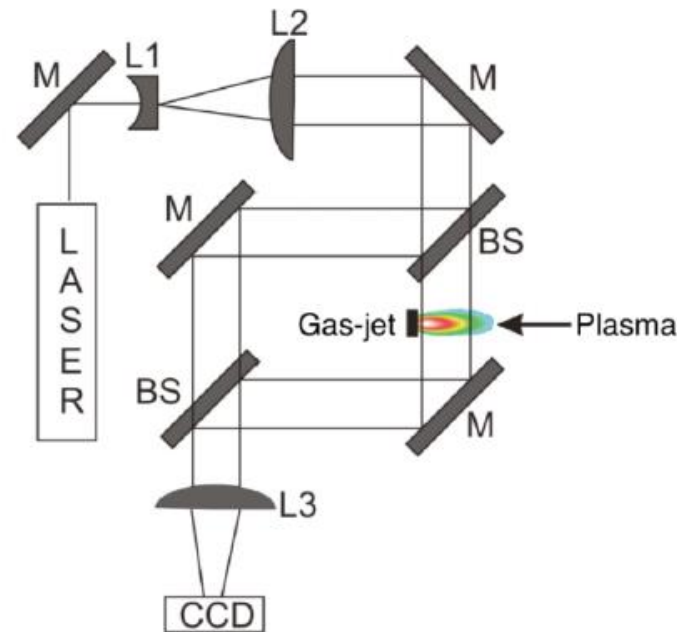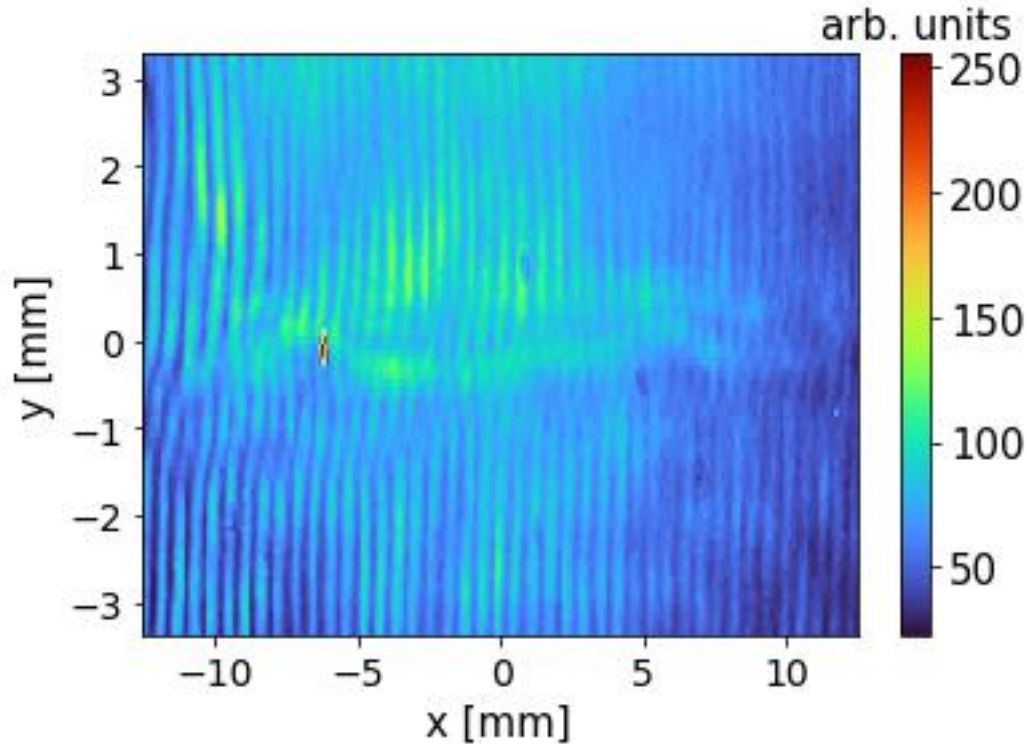
$$\Delta\phi(R,z) = \frac{2\pi}{\lambda n_c} \int_R^{R_0} \frac{r n_e(r,z)}{\sqrt{r^2 - R^2}} dr$$

$$n_e(r,z) = -\frac{\lambda n_c}{\pi} \int_r^{R_0} \frac{d\Delta\phi(R,z)}{dR} \frac{dR}{\sqrt{R^2 - r^2}}$$

We have obtained with a 5 mm long nozzle, with a mix of 10% N 90% He, shooting the laser at 2 mm from the edge of the nozzle a peak electron plasma density of 5x 10^18 cm^-3

Applications: phase-contrast imaging

Imaging
Absorption (ABS) and Phase Contrast (XPCI) mode

$$\eta = 1 - \delta + i\beta$$

ABS

XPCI $\delta \gg \beta$
at high x-ray energies
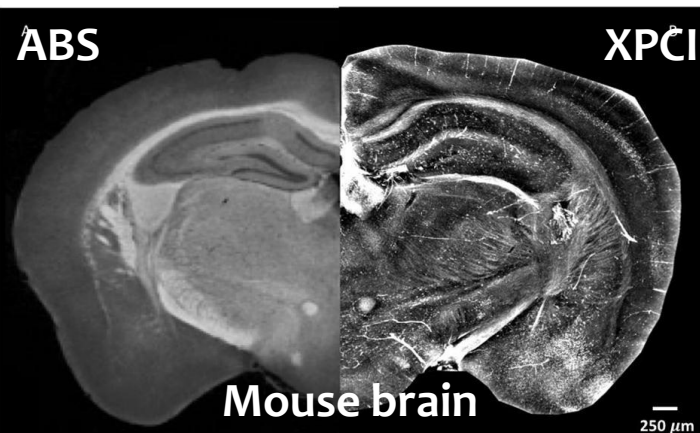
ABS   XPCI

Mouse brain   250 μm

F. Palermo et al. Frontiers in Neuroscience 2020

Need of coherence!

Which coherence?

For betatron radiation sources, that are temporally incoherent, coherence is only spatial

Principles of imaging in transmission: 1D theory

$$\vec{E}(\vec{r}_\perp) = \vec{E}_0(\vec{r}_\perp) e^{-i\omega_0 t + i k_0 z_1}$$

We start with a plane wave, propagating along z
Z1 is the distance between the source and the sample

$$\vec{E}(\vec{r}_\perp) = \vec{E}_0(\vec{r}_\perp) e^{-i\omega_0 t + i k_0 z_1 + i(n(\vec{r}_\perp,\omega_0) + i\kappa(\vec{r}_\perp,\omega_0)k_0 L + i k_0 z_2}$$

Passing through the sample, the phase is modified by the complex index of refraction. Then, the wave propagates from the sample to the detector (distance z2)

$$\vec{E}(\vec{r}_\perp) \simeq \vec{E}_0 e^{-i\omega_0 t + i k_0 (z_1 + z_2)} \left(1 + \overbrace{i n(\vec{r}_\perp,\omega_0) k_0 L}^{\text{Phase Contrast}} - \overbrace{\kappa(\vec{r}_\perp,\omega_0) k_0 L}^{\text{Absorption Contrast}} \right)$$

$$\kappa \ll n$$

For small values of the index of refraction, samples can be «optically» thin, therefore the wave is expressed like this, highligthing two different mechanism of contrast. Moreover we have assumed that the profile of the initial wave is flat, for sake of simplicity.

$$\vec{E}(\vec{r}_\perp) \simeq \vec{E}_0 e^{-i\omega_0 t + i k_0 (z_1 + z_2)} \left(1 + i n(\vec{r}_\perp,\omega_0) k_0 L \right)$$

$$I(\vec{r}_\perp) = I_0 \left[1 + n^2(\vec{r}_\perp,\omega_0) k_0^2 L^2 \right]$$

In phase contrast imaging, absorption is/must be negligible. The wave at the detector plane keeps memory of the index of refraction pattern: phase contrast imaging.

Effect of the sample-detector distance in phase contrast imaging
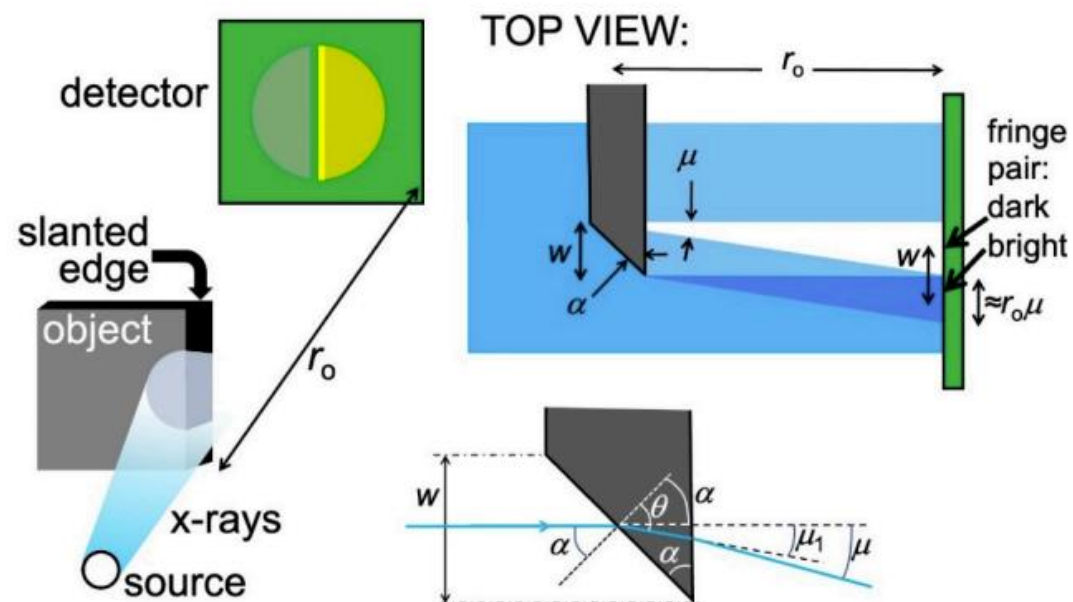
Figure 8. Left: refraction of X-rays passing through a slanted edge between an object and vacuum cause a characteristic pair of bright-fark fringes. A similar phenomenon occurs for a slanted edge separating two different object regions. Top right: analysis of the fringe geometry. Bottom right: enlarged scheme of the edge showing the parameters used ion the analysis.
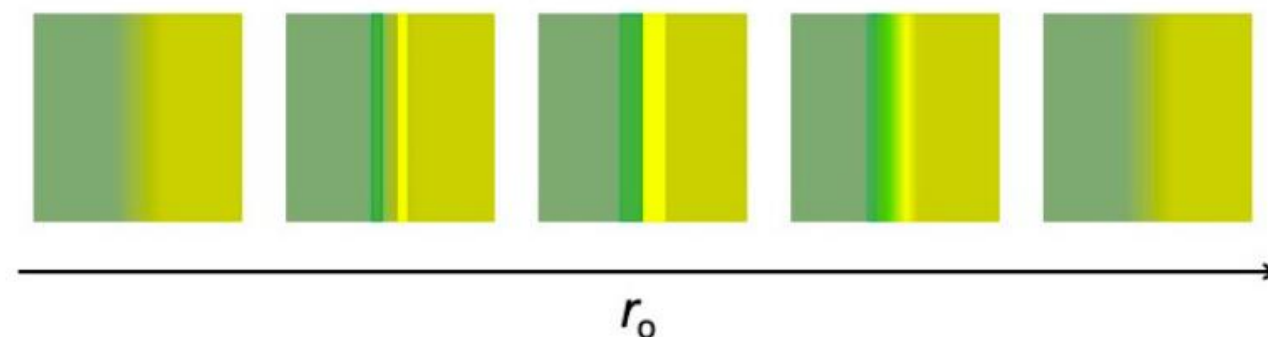
Figure 9. The visibility of a refraction fringe pair changes in a non-monotonic way with the object-detector distance, r_o.

Ref. Margaritondo, Giorgio, and Yeukuang Hwu. "Imaging with coherent X-rays: From the early synchrotron tests to SYNAPSE." *Journal of Imaging* 7.8 (2021): 132.

Attempt of phase contrast image of metallic objects @FLAME
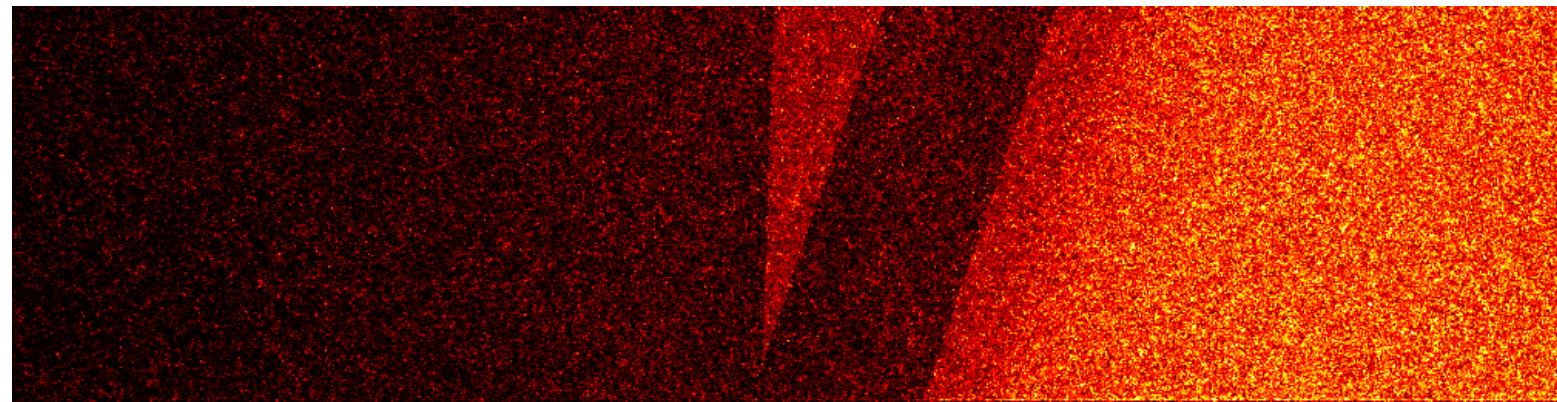
Magnification 1:1, single shot
Resolution 26 um
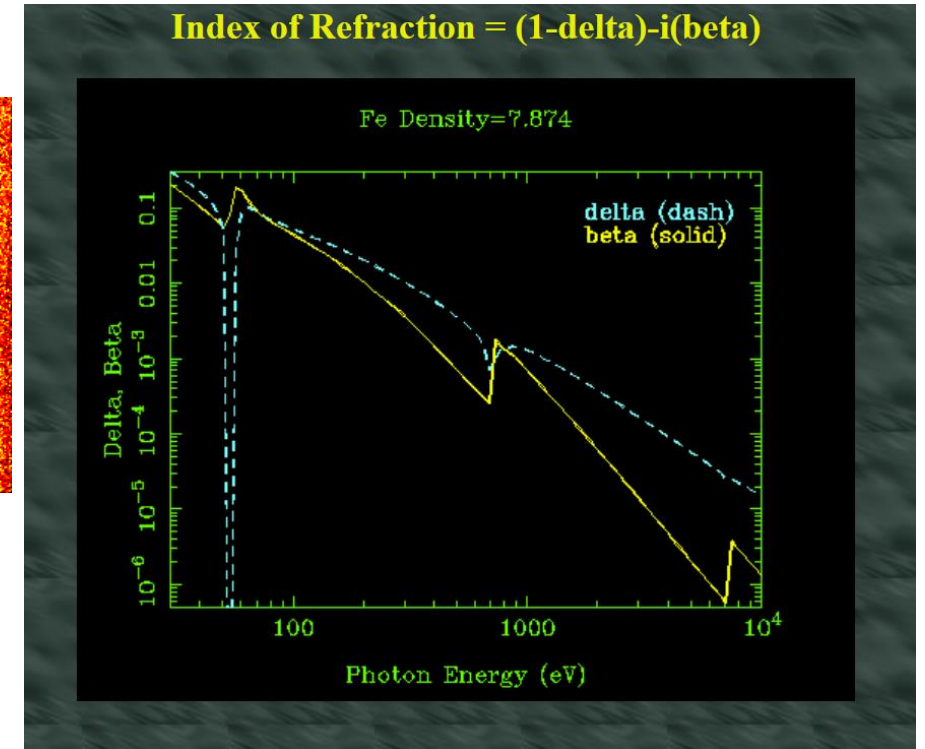
Steel slab covering half sensor (left) and tilted Allen-key on the side (right)

Fish head (detail) and X-ray filter

Al Density=2.6989 Thickness=16. microns
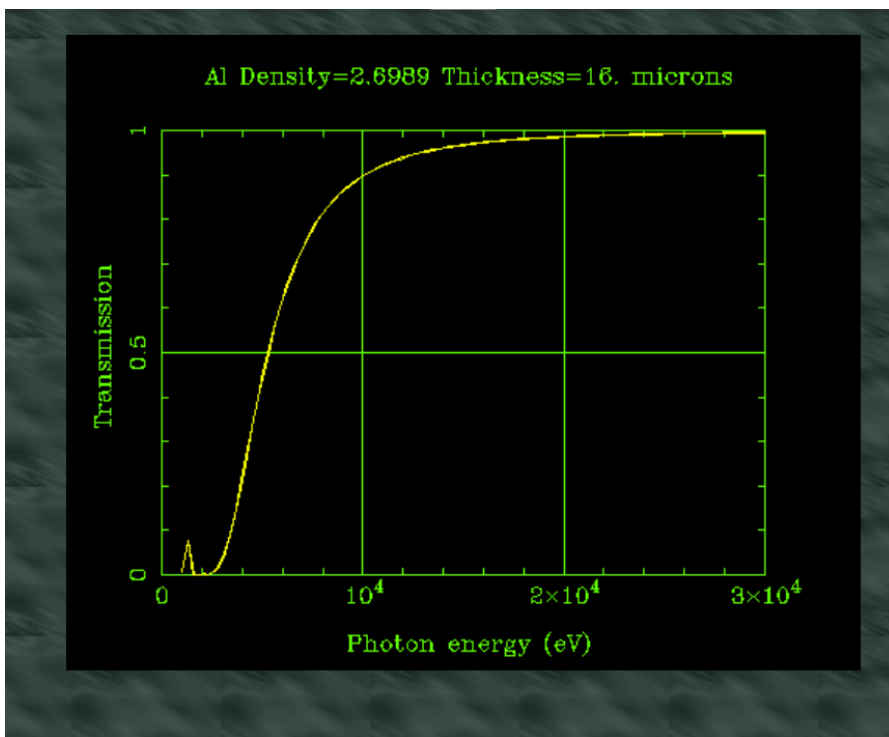
Filter in front of the CCD camera to enhance Phase Contrast and block laser

Irradiated head

Cross-section of the irradiated head

Detail

Attempt of phase contrast imaging of biological objects @FLAME
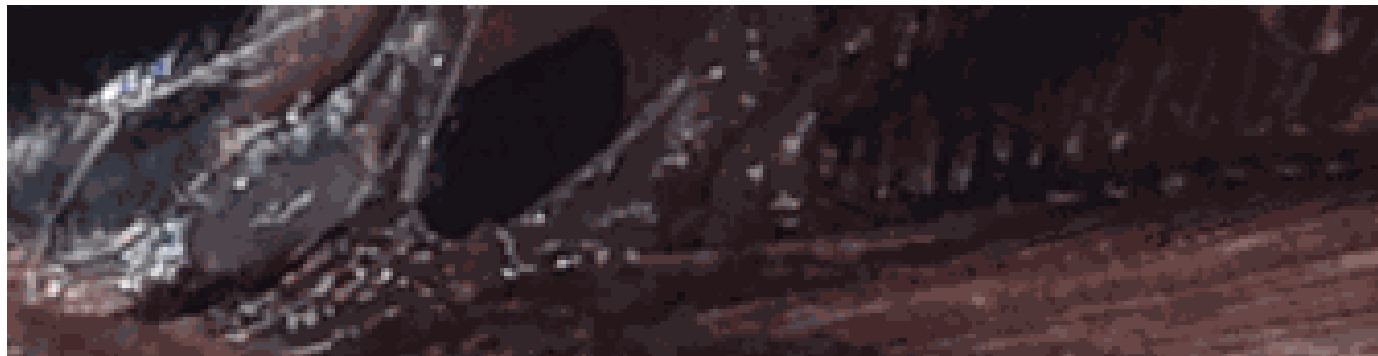
Magnification 1:1, 100 shots accumulated
Resolution 26 um
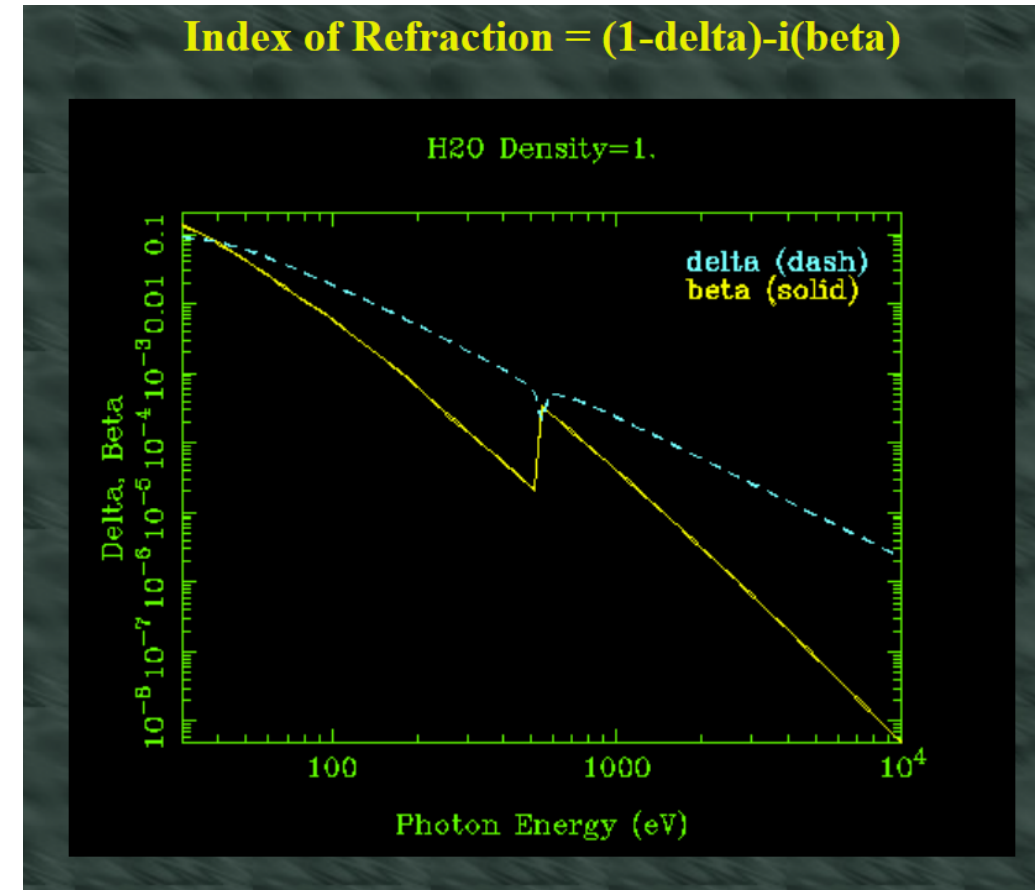
Attempt of phase contrast imaging of biological objects @VEGA

Very similar laser source but 3 meters distance between the object (a spider) and the CCD camera.
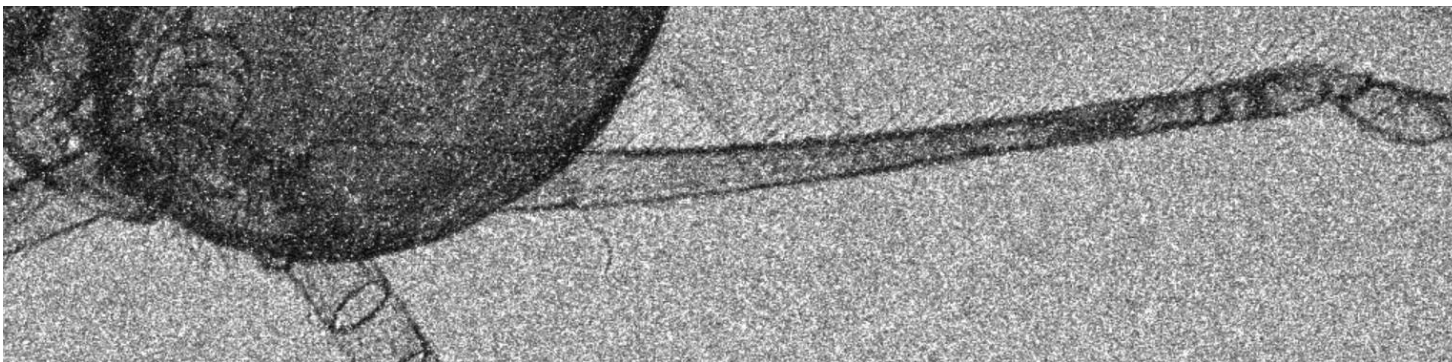
Resolution around 10 um
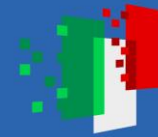
X-ray spectral measurements with absorbers in front of the detector/sensor
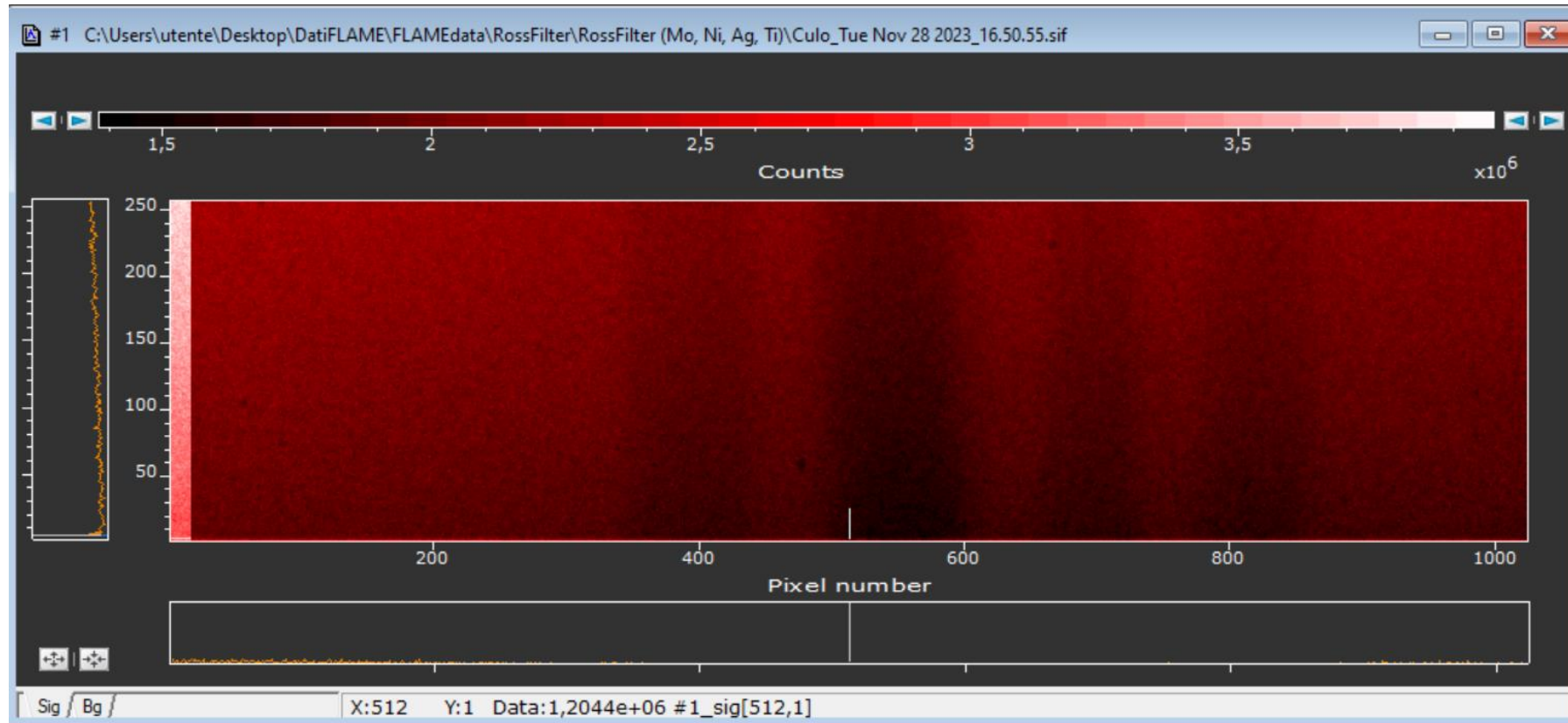
Ti(15um),Ag(33um),Ni(7um),Mo(4um)
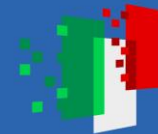
X-ray spectral measurements with absorbers in front of the detector/sensor
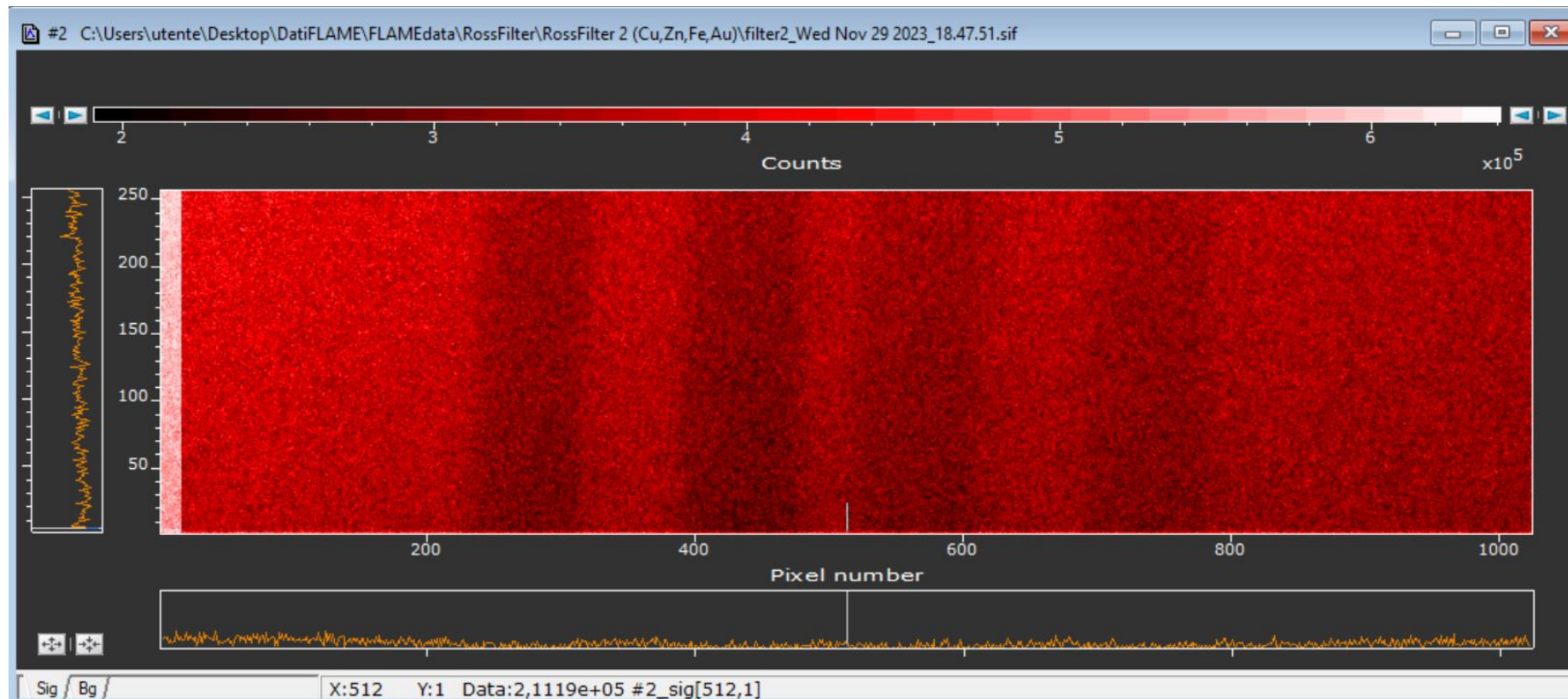
Au(6um),Fe(25um),Zn(10um),Cu(8um)
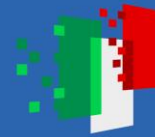
Algorithm for absorption pattern analysis and spectral reconstruction

$$\int \frac{dE}{d\omega} e^{-\alpha_j(\omega)L_j} d\omega \simeq \sum_i \frac{dE}{d\omega}(\omega_i) e^{-\alpha_j(\omega_i)L_j} \Delta\omega_i = I_j$$

The used algorithm is based on the inversion of a linear system of equations, where the index «i» indicates the frequency and the index «j» indicates the absorber.

The above equation is simply the Lambert Beer equation, for the linear absorption of an electromagnetic wave inside a medium characterized by the absorption coefficient alpha and length L.

Ideally, having, an infinite number of absorbers, one can reconstruct the full spectrum.
In the real case with a limited number of absorbers, a fit can be performed.
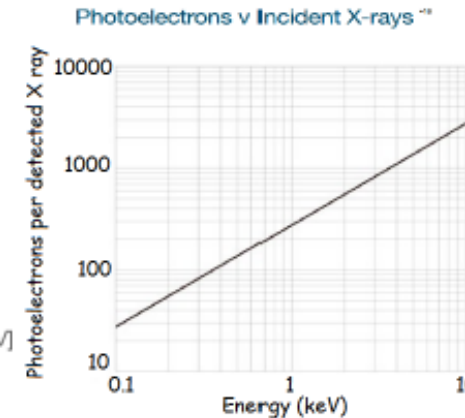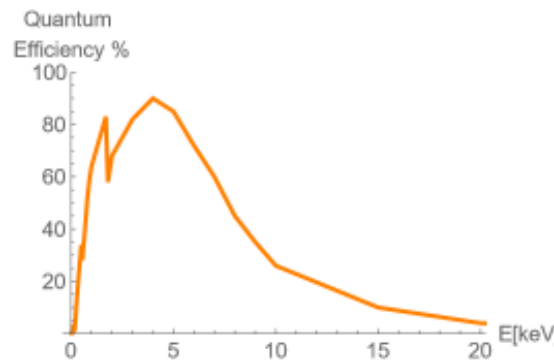
Absorption pattern analysis
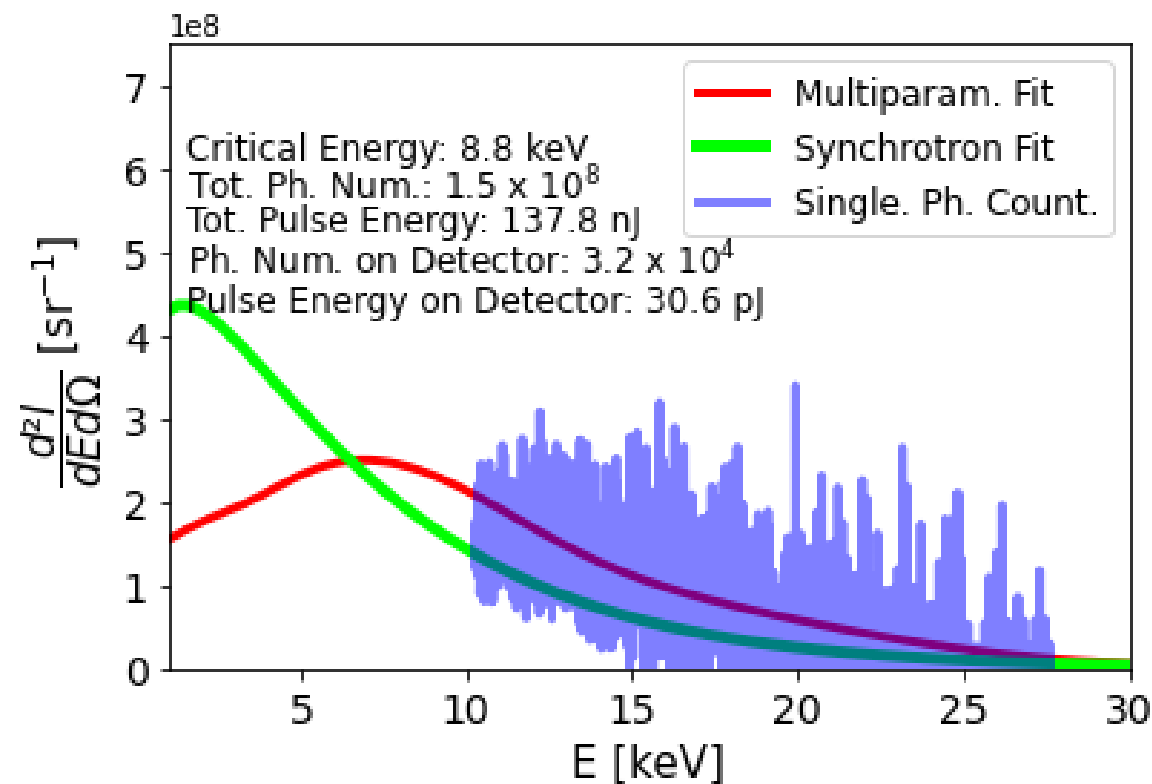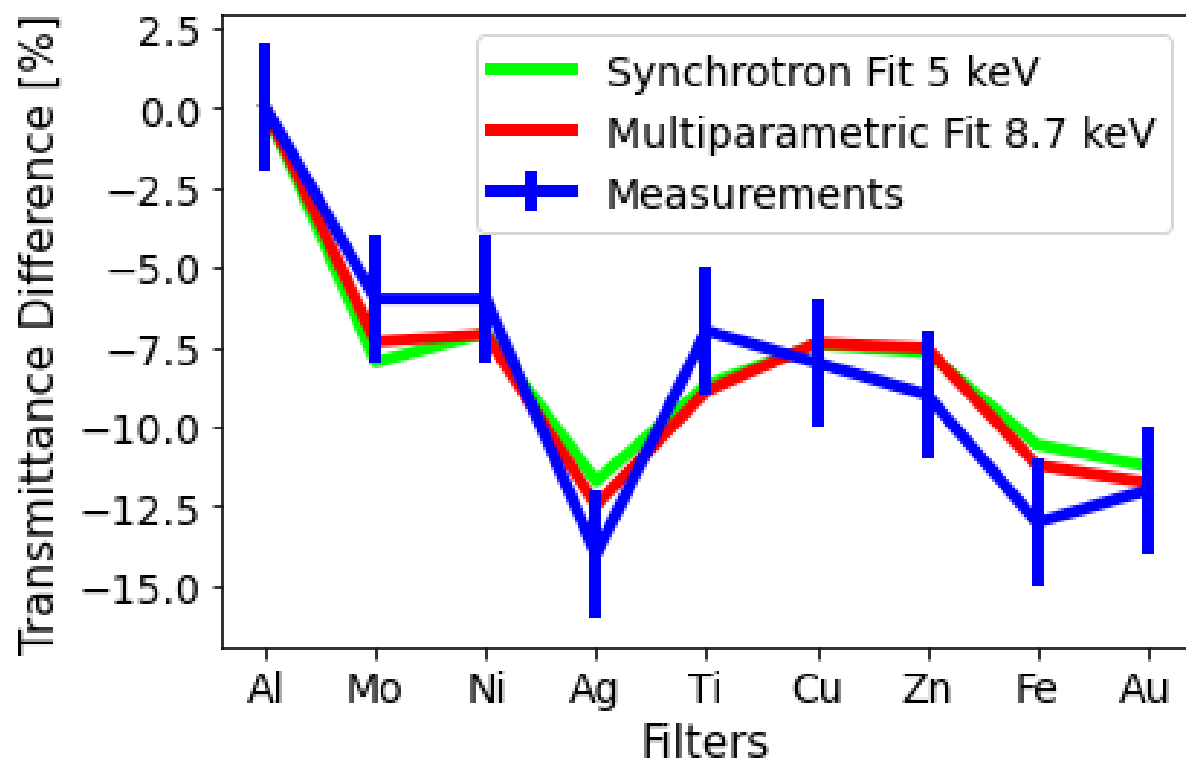
Betatron spectrum detector for single photon counting

Andor DX 434 BR DD

Quantum Efficiency %

Photoelectrons v Incident X-rays

Andor CCD-X for soft X-ray detection together with its quantum efficiency and the number of photoelectrons per detected incident X-ray.

How the raw signal looks like: in single photon counting the histogram of the pixel values is the X-ray spectrum
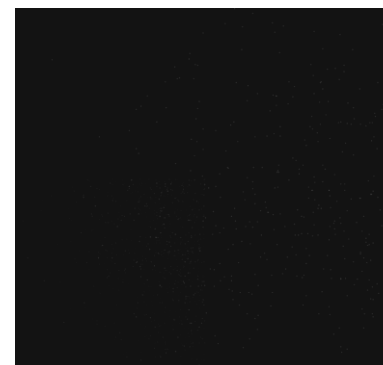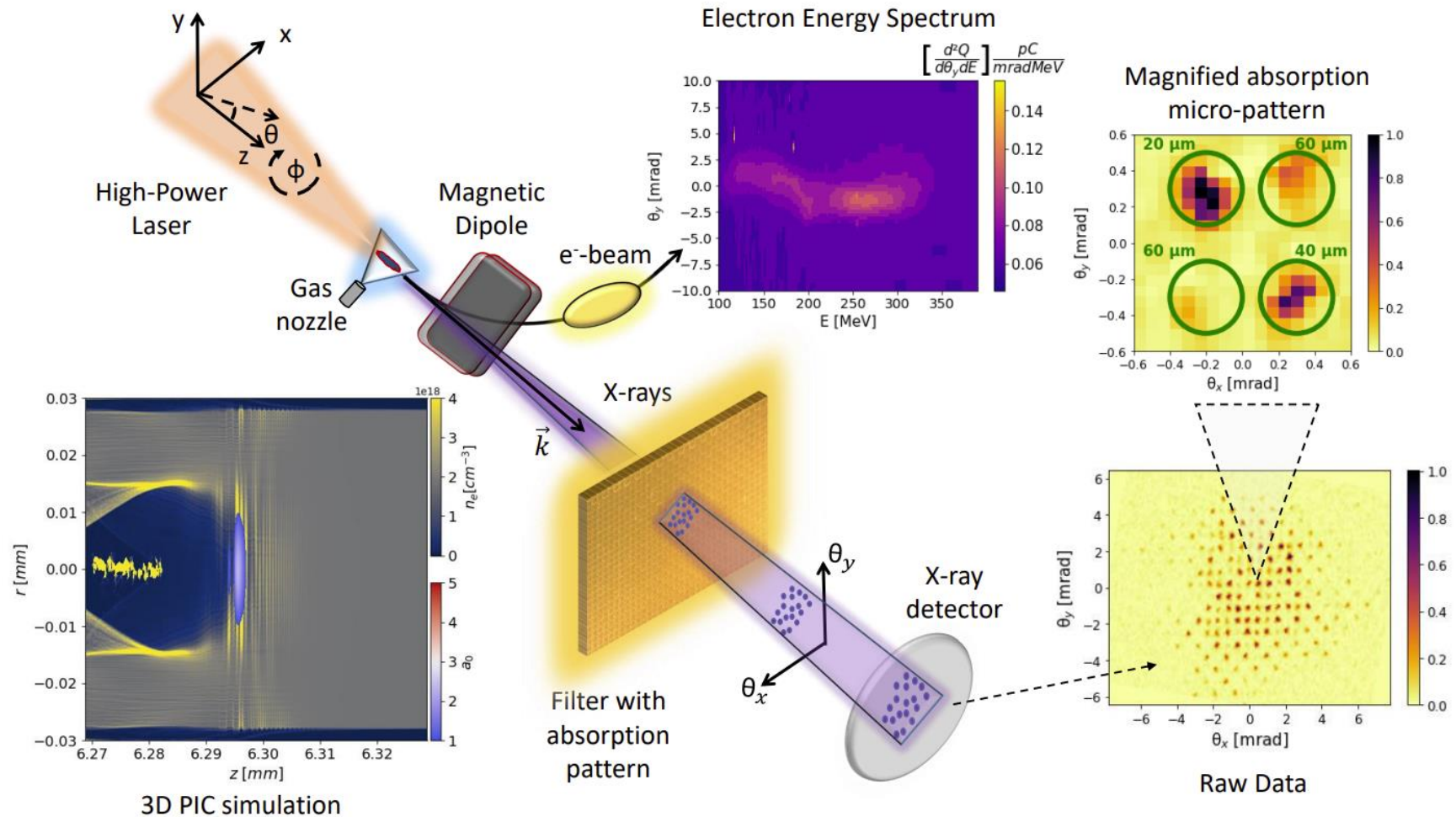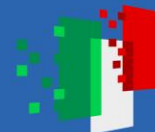
Moving a pinhole across the X-radiation beam: profile measurement
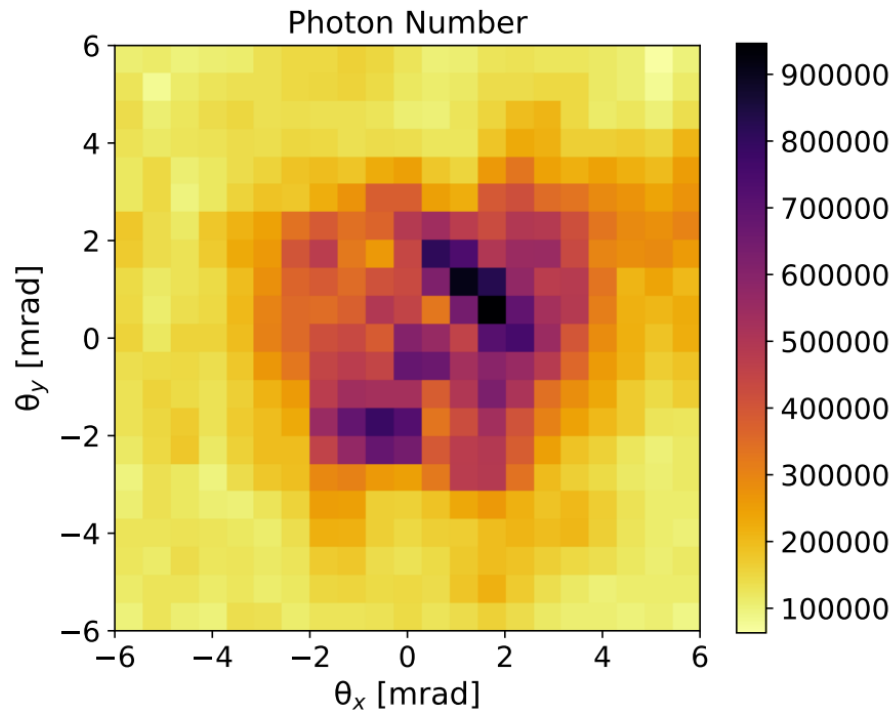
FWHM 60 mrad
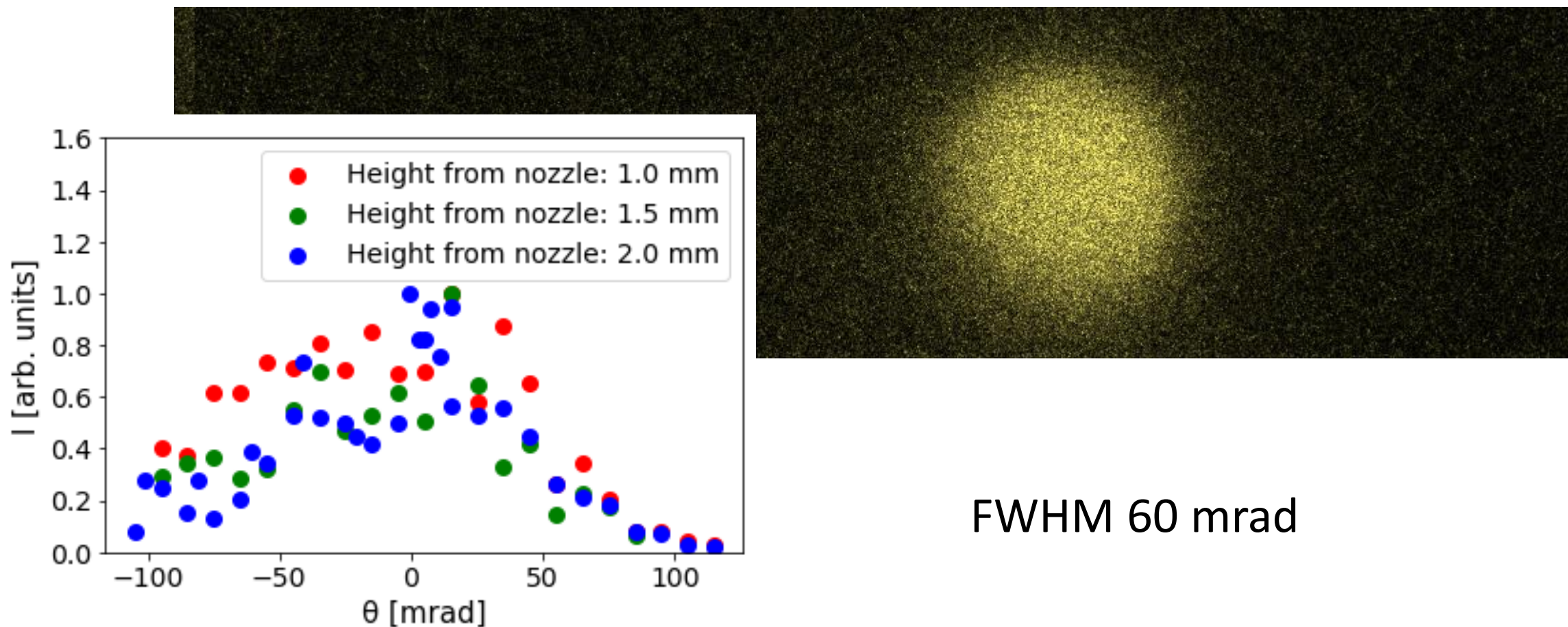
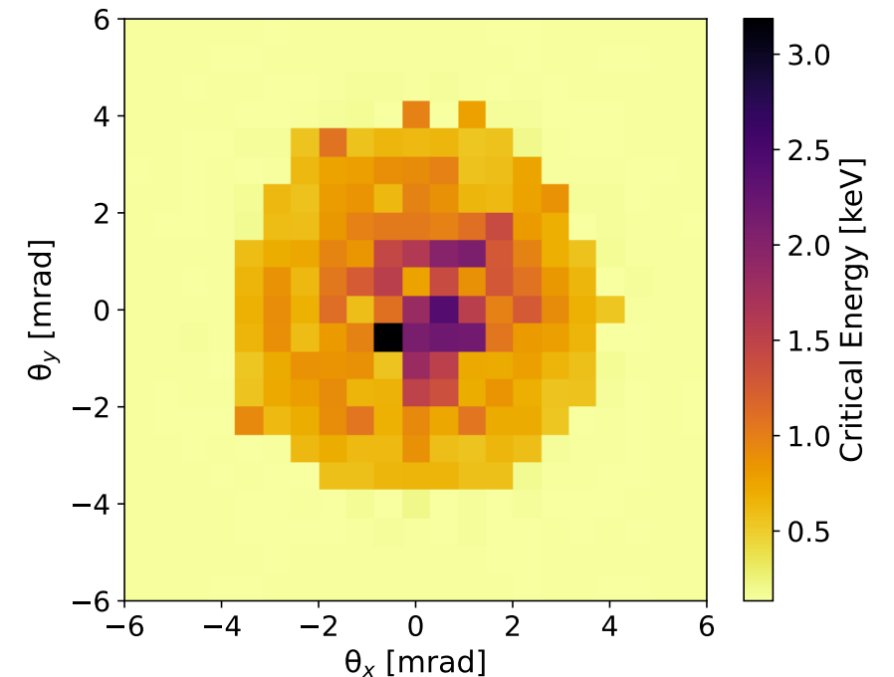# Setup for the measurement of spatial coherence of Betatron Radiation at VEGA 2 (CLPU)

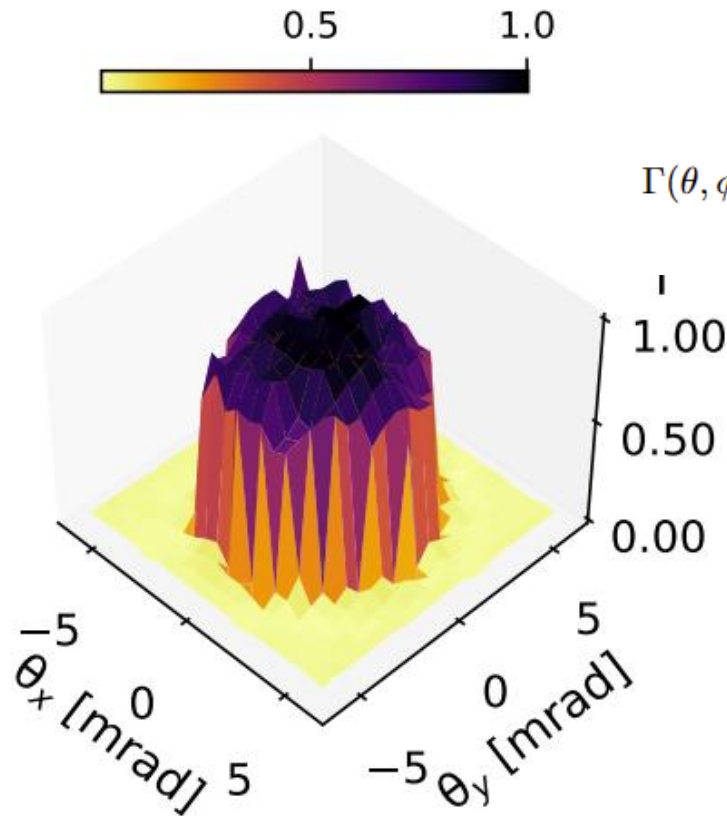# Measurements of Radiation Intensity and Spectral-Angular Distribution

Non-trivial spectral-angular correlation can only be explained with a betatron-phase modulation of the radiation field

$$\vec{H}(t) \propto e^{i\omega t\left[\overbrace{1 - \frac{1}{c}\frac{dz}{dt}\cos\theta}^{On-Axis\ Doppler\ Effect} \overbrace{+ \frac{\omega_\beta}{c}\sin\theta(x_\beta\cos\phi\sin\psi_x + y_\beta\sin\phi\sin\psi_y) - \frac{\omega_\beta^2}{4c^2}\sin\theta\left(x_\beta^2\cos 2\psi_x + y_\beta^2\cos 2\psi_y\right)}^{Betatron\ Phase\ Modulation}\right]}$$
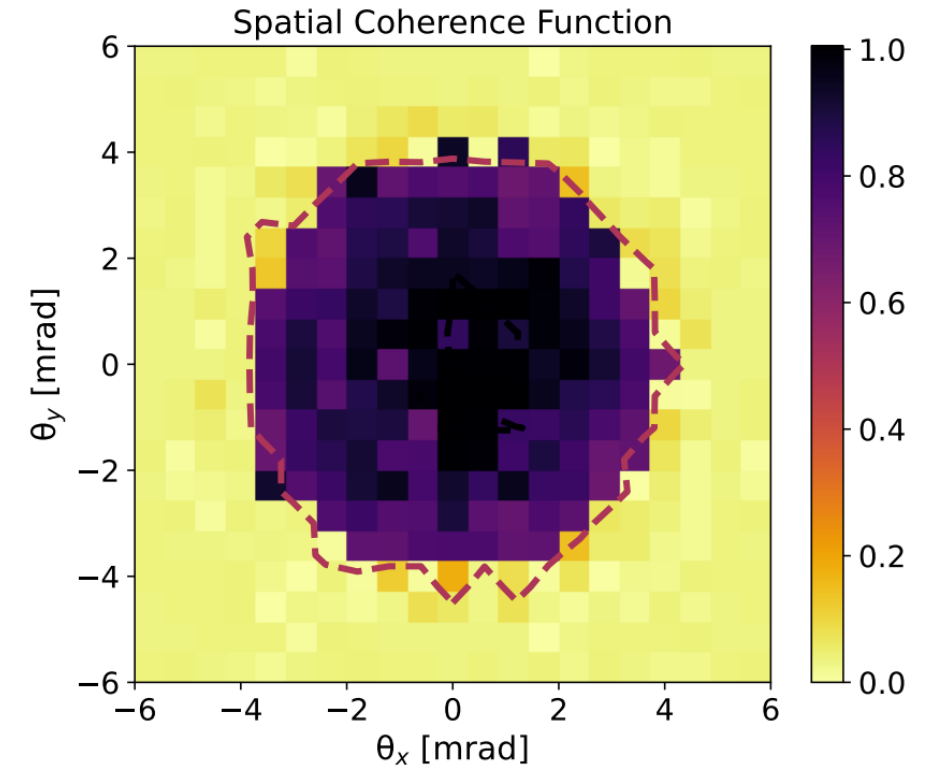
Measurements of Spatial-Coherence

$$\Gamma(\theta, \phi) = \frac{\int d\omega \vec{H}^*(0, 0, \omega)\vec{H}(\theta, \phi, \omega)}{\sqrt{\int d\omega |H(0, 0, \omega)|^2}\sqrt{\int d\omega |H(\theta, \phi, \omega)|^2}}$$

Coherence Function
and
Coherence Area

$$A_c = \frac{\lambda^2}{\pi \sigma_x \sigma_y}$$

Spatial Coherence Function

Ref. Curcio, Alessandro, et al. "Reconstruction of lateral coherence and 2D emittance in plasma betatron X-ray sources." *Scientific Reports* 14.1 (2024): 1719.

Conclusions

- We have introduced the theory of LWFA and betatron radiation

- We have introduced the EuPRAXIA and EuAPS projects

- We have reviewed applications of betatron X-ray sources in view of the realization of a user facility at INFN LNF

- We have reported on the activities of WP2 towards the finalization of the EuAPS project

Alessandro Curcio
acurcio@lnf.infn.it